CHEMISTRY
A EUROPEAN JOURNAL

DOI: 10.1002/chem.200902416

Desymmetrization of 3,3′-Bis(acylamino)-2,2′-bipyridine-Based Discotics: The High Fidelity of Their Self-Assembly Behavior in the Liquid-Crystalline State and in Solution

Michel H. C. J. van Houtem,[a] Rafael Martín-Rapún,[a, b] Jef A. J. M. Vekemans,[a] and E. W. Meijer*[a]

Abstract: Two novel nonsymmetrical disc-shaped molecules **1** and **2** based on 3,3′-bis(acylamino)-2,2′-bipyridine units were synthesized by means of a statistical approach. Discotic **1** possesses six chiral dihydrocitronellyl tails and one peripheral phenyl group, whereas discotic **2** possesses six linear dodecyloxy tails and one peripheral pyridyl group. Preorganization by strong intramolecular hydrogen bonding and subsequent aromatic interactions induce self-assembly of the discotics. Liquid crystallinity of **1** and **2** was determined with the aid of polarized optical microscopy, differential scanning calorimetry, and X-ray diffraction. Two columnar rectangular mesophases (Col_r) have been identified, whereas for C_3-symmetrical derivatives only one Col_r mesophase has been found.[1] In solution, the molecularly dissolved state in chloroform was studied with ^{1}H NMR spectroscopy, whereas the self-assembled state in apolar solution was examined with optical spectroscopy. Remarkably, these desymmetrized discotics, which lack one aliphatic wedge, behave similar to the symmetric parent compound. To prove that the stacking behavior of discotics **1** and **2** is similar to that of reported C_3-symmetrical derivatives, a mixing experiment of chiral **1** with C_3-symmetrical **13** has been undertaken; it has shown that they indeed belong to one type of self-assembly. This helical J-type self-assembly was further confirmed with UV/Vis and photoluminescence (PL) spectroscopy. Eventually, disc **2**, functionalized with a hydrogen-bonding acceptor moiety, might perform secondary interactions with molecules such as acids.

Keywords: chirality · desymmetrization · discotics · liquid crystals · self-assembly

Introduction

Discotics have attracted widespread attention due to their self-organization capabilities in the solid state and in solution. In the solid state they often display columnar liquid crystallinity in which the rigid core of the discotic is organized in one-dimensional columns, whereas the more flexible disordered periphery remains less organized.[2] This behavior greatly enhances their possible application as functional materials in, for example, one-dimensional conductors or photovoltaic cells.[3,4] Self-assembly into nematic mesophases is important for the application in liquid-crystal displays.[5] Apart from π–π stacking,[6] self-assembly driven by hydrogen bonding[7] or coordination[8,9] may give rise to discotic mesophases.[10] In solution, discotics may self-assemble to give fiberlike structures.[11] Often stacks of discotics are helical and, since the helix is an intrinsically chiral object, chirality present in the individual molecule may be transferred to the complete stack at the supramolecular level.[12] Hydrogen bonding may be a major driving force for columnar, helical stacking as is the case for small *N*,*N*′,*N*″-trialkyl benzene-1,3,5-tricarboxamide (BTA) discs in which the amide functionality is involved in a threefold helical array of intermolecular hydrogen bonding.[13,14] More than a decade ago, we described a specific kind of discotic mesogens based on the BTA core, **A** (Figure 1a), which possesses a large central core resulting from amidation of 1,3,5-benzenetricarbonyl trichloride with three monoacylated 2,2′-bipyridine-3,3′-di-

[a] M. H. C. J. van Houtem, Dr. R. Martín-Rapún, Dr. J. A. J. M. Vekemans, Prof. Dr. E. W. Meijer
Laboratory of Macromolecular and Organic Chemistry
Eindhoven University of Technology
P.O. Box 513, 5600 MB Eindhoven (The Netherlands)
Fax: (+31) 40-245-1036
E-mail: E.W.Meijer@tue.nl

[b] Dr. R. Martín-Rapún
Current address: Institute of Chemical Research of Catalonia
Av. Països Catalans, 1643007 Tarragona (Spain)

Supporting information for this article is available on the WWW under http://dx.doi.org/10.1002/chem.200902416.

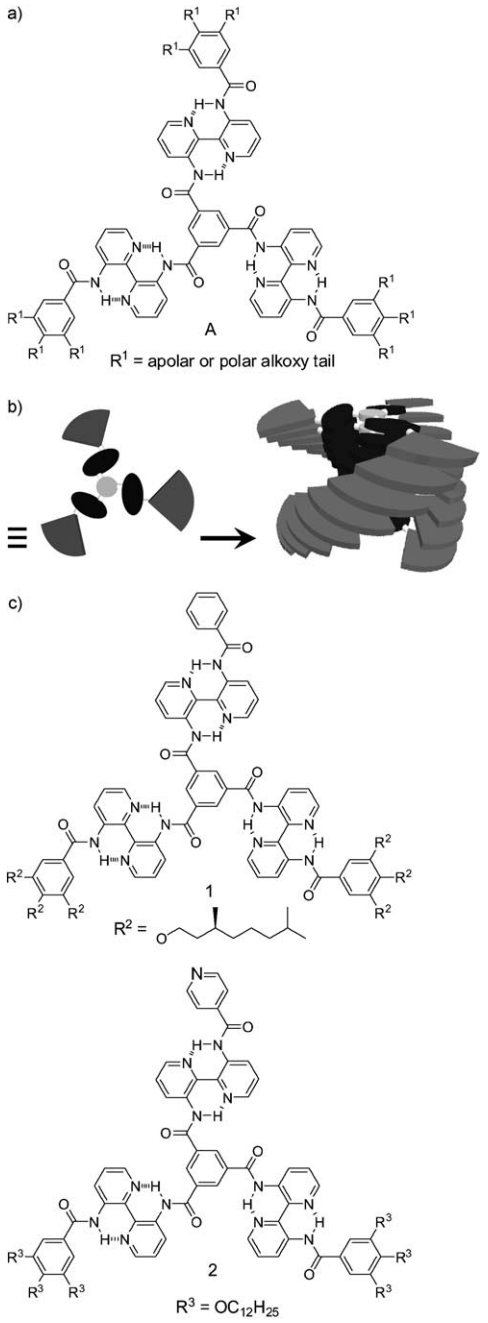

Figure 1. a) C_3-symmetrical discotics **A** with a benzene core and equipped with three 3,3′-bis(acylamino)-2,2′-bipyridine moieties and nine nonpolar (R = O–alkyl)[16] or polar (R = O–oligo(ethylene oxide))[18] alkoxy peripheral tails. b) Their helical self-assembly depicted as a drawing. c) Chiral, nonsymmetric benzene discotic **1** and achiral, nonsymmetric pyridine discotic **2**. Intramolecular hydrogen bonding is represented with dashed lines.

amine moieties.[15] Strong intramolecular hydrogen bonding between amide N–H groups and bipyridine N atoms preorganizes the molecule into a C_3-symmetrical conformation that is, on average, planar.[16] Stacking due to mainly aromatic interactions occurs in the solid state and in dilute solution. In these self-assemblies the discotics adopt a propeller-like conformation to afford helicity (Figure 1b). The nine peripheral alkoxy tails induce phase separation and solubility and they determine the polarity of the compounds. In the solid state, columnar liquid crystallinity is present over a very broad temperature window (>300 K) provided long peripheral tails are present. In solution, these tails ensure solubility and allow the introduction of chirality into the system.[17] Bipyridine-based discotics equipped with polar oligo(ethylene oxide) tails have also been described as displaying solubility and expressing chirality in aqueous media as well as mesophase formation.[18,19] Both apolar and polar bipyridine-based discotic systems obey in dilute solution the "sergeant and soldiers" principle,[17,20,21] and the apolar discotics also obey the "majority rules",[22] both proposed by Mark Green et al. for covalent polymers.

Possible applications for these discotics are emerging.[19,23] Our aim is to widen the applicability of these star-shaped 3,3′-bis(acylamino)-2,2′-bipyridine discotics in supramolecular systems by replacing one of the trialkoxyphenyl moieties with a functional unit. Such a unit would allow interaction with other compounds with the goal of influencing liquid-crystalline behavior to introduce chirality by secondary interactions and performing covalent or supramolecular fixation of the discotic assembly. Numerous nonsymmetric discotics have been described with the aim of altering mesophase properties and transitions,[14,24] thereby allowing interactions and functionality in the mesophase[25] or producing discotic mesogens with special optical properties.[26] In solution, desymmetrized, amphiphilic hexabenzocoronenes, which are designed to self-assemble into chiral, helical tapes and nanotubes are well known,[27] as are nanofiber-forming amphiphilic, ionic hexabenzocoronenes.[28] Some desymmetrized discotics are prone to covalent[29,30] or even supramolecular[31] fixation.

In this paper, the synthesis and the characterization in the mesophase and in solution of two nonsymmetric discotics **1** and **2** (Figure 1c) are described. The main question is whether these desymmetrized molecules adopt similar discotic structures and self-assemblies in the mesophase and in solution as previously reported C_3-symmetrical analogues. If so, in the case of disc **2**, introduction of functionality into these discotic systems will be possible. In both discotics **1** and **2**, one trialkoxyphenyl wedge has been replaced by the smaller phenyl and 4-pyridyl moieties, respectively. Discotic **1**, equipped with chiral dihydrocitronellyl tails, is relevant since its chirality allows its stacking properties to be studied with chiral-optical techniques like CD spectroscopy. Discotic **2** incorporates a basic pyridyl group that affords functionality to the discotic system, thereby allowing interactions with other compounds and supramolecular fixation of the self-assembled stacks.

Results and Discussion

Synthesis of chiral benzene discotic 1: The synthesis of nonsymmetric discotic **1** was performed as depicted in Scheme 1. This statistical synthesis relies on two different ar-

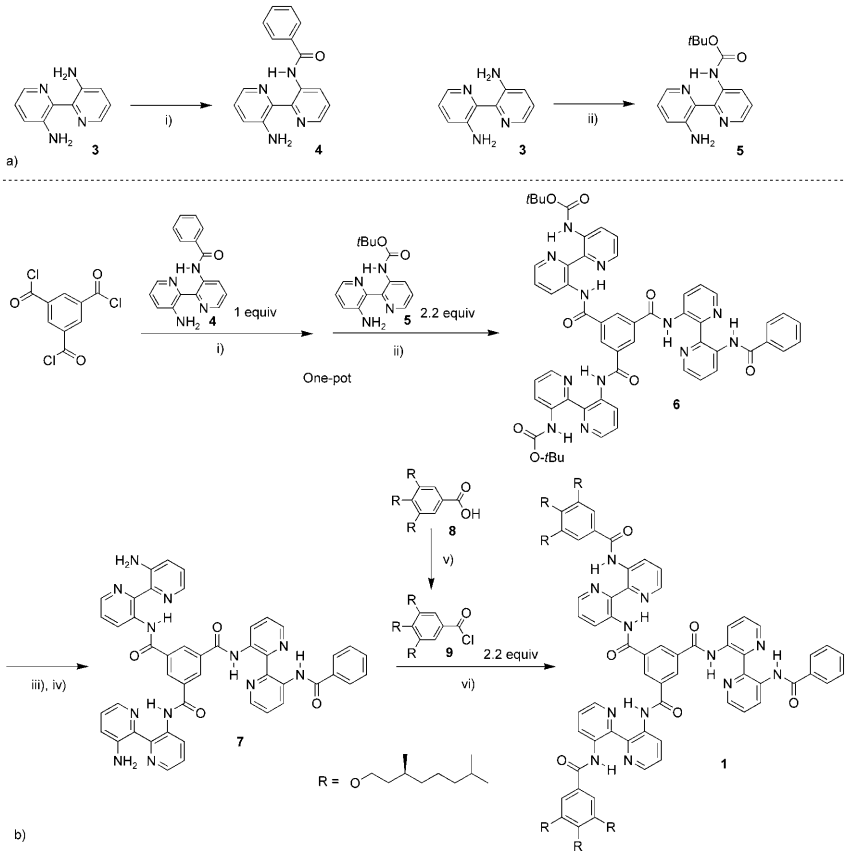

Scheme 1. a) Synthesis of monoacylated compounds **4** and **5**: i) benzoyl chloride (1.1 equiv), TEA, CH_2Cl_2, 0 °C→RT, 28 h; ii) di-*tert*-butyl dicarbonate (1.2 equiv), ethanol, 35 °C, 5.5 h. b) One-pot reaction towards nonsymmetric compound **6** followed by deprotection of the Boc groups and subsequent acylation with chiral, mesogenic acid chloride **9**: i) DIPEA, CH_2Cl_2, 10 °C→RT, 3 h; ii) DIPEA, CH_2Cl_2, 10 °C→RT, 17 h; iii) TFA, CH_2Cl_2, 0 °C→RT, 5 h; iv) TEA, acetone, 10 min; v) $SOCl_2$, DMF, CH_2Cl_2, RT, 17 h; vi) DIPEA, *N*-methyl-2-pyrrolidone, 17 h.

omatic amines **4** and **5** that consecutively were reacted with trimesyl chloride to afford nonsymmetrical precursor **6** in one step (Scheme 1b). Aromatic amines **4** and **5** were obtained by reacting 2,2′-bipyridine-3,3′-diamine (**3**) with one molar equivalent of an acid chloride or anhydride (Scheme 1a).[15] The synthesis of *tert*-butoxycarbonyl (Boc)-protected **5** was slightly adjusted due to the low reactivity of poorly nucleophilic **3** towards di-*tert*-butyl dicarbonate.[32] Deactivation of the second amino functionality of **3** due to intramolecular hydrogen bonding and concomitant planarization ensured highly selective monoacylation.[16] In the first reaction step of the one-pot reaction, one molar equivalent of aromatic amine **4** was added slowly to trimesyl chloride to obtain, on average, monoacylation (Scheme 1b) subsequently followed by addition of an excess of Boc-protected aromatic amine **5** to ensure complete amidation of the remaining acid chloride functionalities. The Boc groups of compound **6** allow incorporation of any alkylated wedge after deprotection with trifluoroacetic acid (TFA). The one-pot synthesis of **6** was relatively easy to carry out, but had the disadvantage that the purification of the statistical mixture to afford pure **6** was quite tedious due to comparable polarities and hydrodynamic volumes of the tertiary butyl group and the phenyl group. Also, stacking of the different components when present in concentrated solution during chromatographic purification hampers their efficient separation. Analytical GPC[33] did not show a difference in retention time between the different components. Eventually, the purification was performed in two steps. Precipitation in a polar solvent in which desired product **6** does not dissolve allowed the removal of unreacted mono-protected amine **5** and *N*,*N*-diisopropylethylamine (DIPEA) salts by simple filtration. Then the crude product was further chromatographically purified with a chloroform/pyridine mixture as the eluting solvent to minimize stacking. However, according to ^{1}H NMR spectroscopy and MALDI-TOF mass spectrometry, some impurities remained. The Boc groups of intermediate product **6** were removed by TFA in dichloromethane followed by neutralization with triethylamine (TEA). Surprisingly, the TFA salt is soluble in dichloromethane and acetone, whereas the neutralized product **7** is not (Scheme 1b). The limited solubility of this neutralized product **7** required polar *N*-methyl-2-pyrrolidone as solvent in the final reaction step in which it was reacted with chiral acid chloride **9**. The latter acid chloride was obtained from the corresponding carboxylic acid **8** according to a slightly modified literature procedure,[16,30,34] whereas carboxylic acid **8** was obtained according to established procedures.[16] Precipitation of the reaction mixture in polar solvent and column chromatography gave pure, nonsymmetric discotic **1**. Based on amino precursor **4**, the overall yield amounted to 14%.

Synthesis of achiral pyridyl discotic 2: The synthesis of nonsymmetric, functionalized discotic **2** has been performed with an adjusted statistical method in which the alkylated wedges were directly incorporated, thereby allowing the final separation step to be based on hydrodynamic volumes (Scheme 2). Recycling gel permeation chromatography (GPC) proved to be an effective method to purify discotics equipped with bulky alkylated wedges; the side products either lack or have an excess of three long alkoxy tails or even a complete 3′-(3,4,5-trisalkoxybenzoylamino)-2,2′-bipyridyl-3-amine wedge. The synthesis of 4-pyridyl-function-

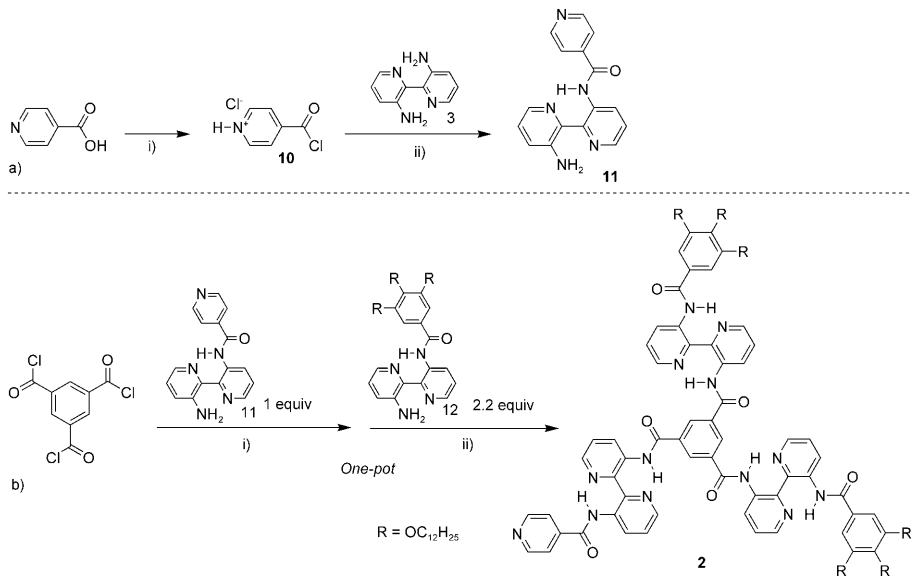

Scheme 2. a) Synthesis of 4-pyridyl-functionalized aromatic amine **11** starting with isonicotinic acid: i) thionyl chloride, 76 °C, 5 h; ii) DIPEA, CH_2Cl_2, 0 °C→RT, 5 h. b) One-pot reaction to obtain nonsymmetric, achiral discotic **2** in only two steps from their aromatic amine precursors **11** and **12**: i) DIPEA, CH_2Cl_2, 10 °C, 10 min; ii) DIPEA, CH_2Cl_2, 10 °C→RT, 3 h.

alized aromatic amine precursor **11** is shown in Scheme 2a. Pyridine-4-carbonyl chloride HCl salt (**10**) was synthesized by reacting isonicotinic acid in hot thionyl chloride.[35] The obtained acid chloride was subsequently reacted with **3** by slow addition of **10** to **3** to prevent diacylation and maximize product formation.[15] The synthesis of hydrophobic aromatic amine precursor **12** has been reported previously.[16] In a one-pot reaction, amines **11** and **12** were added successively to a solution of trimesyl chloride to afford disc **2** together with its statistically determined analogues. Chromatographic purification as described above yielded pure disc **2** in a yield of 12% based on amino precursor **11**.

Liquid-crystalline behavior of discotics 1 and 2: Both nonsymmetric discs **1** and **2** are sticky solids at room temperature, as are the majority of C_3-symmetrical analogues that display a very broad liquid-crystalline window of more than 300 K.[16] The mesogenic properties of both discotics **1** and **2** were determined using differential scanning calorimetry (DSC), polarizing optical microscopy (POM), and X-ray diffraction (XRD). The influence of the adaptation, in which a bulky, alkylated group is replaced by a small, rigid group on the liquid-crystalline properties of discotics **1** and **2** is of especial interest. Thermal gravimetric analysis (TGA) (see Figure S1 in the Supporting Information) was used to determine the thermal stability of discotic **1**. Compound **1** displays no degradation below 350 °C under a nitrogen atmosphere. However, severe decomposition starting from 300 °C was observed when TGA was performed under an oxygen-rich atmosphere. Therefore, DSC and POM were conducted under a nitrogen atmosphere to ensure reliable results. The DSC measurements of discotics **1** and **2** are shown in Table 1.

Table 1. DSC data for the phase transitions of discotics **1** and **2**.[a]

First cooling run (10 °C min^{-1})[b]				Second heating run (10 °C min^{-1})[b]			
Compd	T_{onset} [°C]	ΔH [kJ mol^{-1}]	Phase transition[c]	Compd	T_{onset} [°C]	ΔH [kJ mol^{-1}]	Phase transition[c]
1	329	6	I–LC	**1**	328	6	LC–I
	201	9	LC–LC		203	10	LC–LC
2	336	6	I–LC	**2**	335	7	LC–I
	206	10	LC–LC		215	11	LC–LC
	−3	38	LC–Cr		3	42	Cr–LC

[a] Measurements were conducted between −50 and 350 °C. The onset was taken for the transition temperatures. [b] Heating and cooling runs at a rate of 10 K min^{-1} are given in Figures S2 and S3 of the Supporting Information. [c] Type of phase transition according to POM. Exact mesophase was determined with XRD. LC = liquid crystalline; Cr = crystalline.

DSC and polarizing optical microscopy: For compounds **1** and **2** in both DSC and POM, a transition to the isotropic melt at about 325 °C was observed that allowed the growth of liquid-crystalline textures under the microscope by slow cooling to confirm the mesogenic properties of the compounds. The enthalpy values associated with the clearing point are on the same order of magnitude as that of similar C_3-symmetrical discotics.[16] Depicted in Figures 2 and 3 are the pseudo-focal-conic textures, typical of columnar mesophases, exhibited by discs **1** and **2** in the mesophase below the isotropization temperature.[36] The straight lines present in the textures are indicative of an ordered columnar mesophase.[37] Interestingly, a transition to a lower temperature mesophase was detected by DSC for both **1** and **2** at approximately 200 °C. This transition is not present in their symmetrical analogues.[16] Apparently, it does not matter whether a phenyl or pyridyl group replaces the trialkoxyphenyl wedge in **1** and **2** for the appearance and thermal position of the transition between the two mesophases. Also, this transition temperature between two mesophases is not influenced by a branching of the aliphatic tails. The enthalpy values associated with this transition are relatively small, which means that there is no large structural difference between the two mesophases of **2** and **3**. The transition between the two mesophases can actually consist of a two-step transition, as is supported by the presence of two peaks in the DSC run of disc **1** (see the Supporting Information, Figure S2).[38] This transition was observed by POM for discs **1** and **2** as a rapid change of the texture around 210 °C,[39] while the compound remained fluidic under pressure (Figures 2b and Figure 3b). The discotics display a very broad

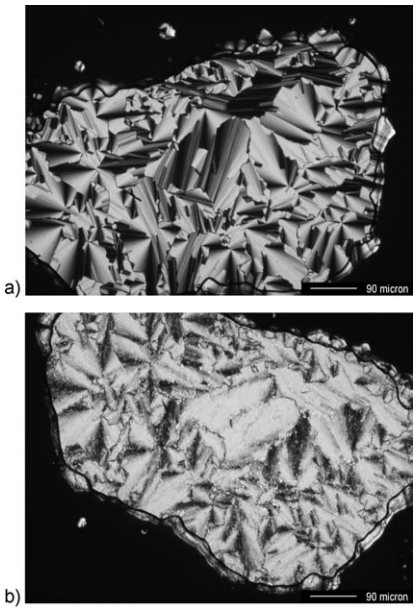

Figure 2. Polarized optical micrographs of discotic **1** at a) 295 and b) 175 °C (same area, rotated).

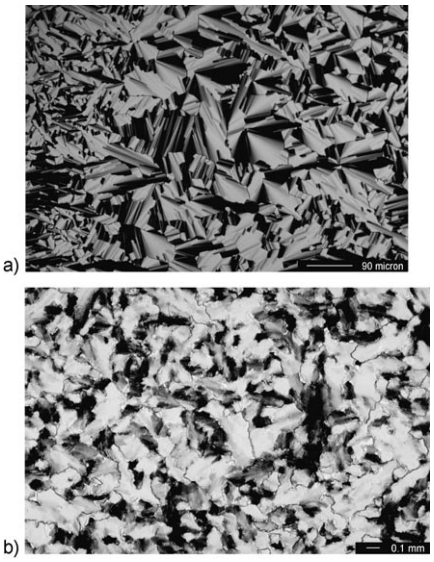

Figure 3. Polarized optical micrographs of discotic **2** at a) 315 and b) 160 °C (same area).

liquid-crystalline window (> 300 K) and are liquid crystalline at room temperature, which is important for future applications.[3] Apparently, the removal of one trialkoxy group compared to their C_3-symmetrical analogues does not decrease the ability of discotics **1** and **2** to form mesophases. Below room temperature, discotic **2** exhibits a liquid-crystalline to crystallization (LC–Cr) transition. Although the observed texture undergoes only very subtle changes, we assign the transition as crystallization as it is accompanied by a large enthalpic change relative to the transitions at approximately 200 °C and 325 °C. For compound **1** no melting transition was observed. The absence of a melting point is probably due to the presence of branched side tails in compound **1** that will lower the melting point.[40] The isotropic transitions of both discs **2** and **3** are lower than that of related nonpolar discotics **A** (Figure 1a), which is in agreement with other reported desymmetrized systems.[41] All discussed phases in discotics **1** and **2** are enantiotropic and little hysteresis was observed for the LC–LC transitions at approximately 200 °C for both **1** and **2** and for the Cr–LC transition of discotic **2** (see Figures S2 and S3 of the Supporting Information for the DSC plots).

X-ray diffraction: The two discotics **1** and **2** were investigated by small- (SAXD) and wide-angle (WAXD) X-ray diffraction with the aim of verifying the type of mesophase and to determine the structural parameters. As seen in the DSC traces, the structures of the mesophases at room temperature (RT) and above are equivalent for both compounds. Below RT an additional phase was detected for discotic **2**, and for that reason the results for discotic **2** will be discussed in particular. All SAXD and WAXD data for both discotics **1** and **2** are gathered in Table 2.

The WAXD profile of discotic **2** at RT (Figure 4a) exhibits two features in the large-angle region. One peak corresponds to a distance of 3.3 Å, which is in the range of the stacking distance between aromatic rings in the liquid-crystalline state. This confirms the ordered columnar structure of the phase. The other feature is a diffuse halo that corresponds to a distance of about 4.5 Å, the typical distance between molten alkyl chains in a mesophase.[42] These features remained present up to the maximum temperature limit of 200 °C of the WAXD setup. Upon cooling from RT to −21 °C, the alkyl chains freeze in a more ordered or crystalline phase, and the diffuse halo turned into a peak that corresponded to 4.2 Å.

SAXD patterns of discotic **2** at −21 °C and RT are analogous and display a set of maxima with an additional peak at the lower temperature (Figure 4b). The ratio between the spacings that correspond to the peaks is not a reciprocal ratio indicative of square or hexagonal two-dimensional lattices. However, they can be indexed according to a rectangular symmetry *P2gg* based on the extinction rules. The lattice parameters of the rectangular arrangement are given in Table 2. The phase at −21 °C has the same structure as the liquid-crystalline phase at RT, except for the peripheral alkyl chains, which are crystallized in the columnar rectangular mesophase Col_{r1}. Upon an increase in temperature, a third phase Col_{r3} appeared. The SAXD profile at 240 °C is simpler than the profiles at lower temperatures. Only three peaks are present in the small-angle region, which can be indexed according to a rectangular symmetry too. Nevertheless, the unit cell for this Col_{r3} phase is much smaller than for the lower temperature phases (Table 2). As commented above, WAXD data unfortunately were not available for this phase. In a columnar rectangular phase, there are typically two columns per unit cell, one of which is in the center, and the other is in the corner of the unit cell. This is the case for the Col_{r3} phase, which exhibits similar lattice pa-

Table 2. X-ray results for the mesophases of nonsymmetrical discotics **1** and **2**.

Compound	T [°C]	Phase	$h\,k\,l$	d_{obsd} [Å][a]	d_{calcd} [Å]	Lattice constants [Å]	ρ_{calcd} [g cm^{-3}][b]
discotic **1**	RT	Col_{r2}	2 0 0	50.3	50.3	$a=100.5$	0.91
		P2gg	1 1 0	34.5	34.5	$b=36.8$	
			4 0 0	25.4	25.1	$c=38.0$[c]	
			0 2 1	16.6	16.6	$h=3.3$	
			2 2 1	15.8	15.7	$Z=4$[d]	
			4 2 1	14.4	14.8		
			7 1 0	13.3	13.4		
			alkyl	4.5 (br)	–		
			π–π	3.3	–		
	230[e]	Col_{r3}	2 0 0	34.7	34.7	$a=69.4$	0.93
		C2mm	1 1 0	29.8	29.8	$b=33.0$[c]	
			0 2 0	16.5	16.5	$Z=2$[d]	
discotic **2**	−21	Col_{r1}[f]	2 0 0	53.3	53.3	$a=106.6$	0.98
		P2gg	1 1 0	38.0	38.0	$b=40.6$	
			2 1 0	32.5	32.3	$c=36.5$[c]	
			3 1	26.4	26.6, 26.7	$h=3.3$	
			0, 4				
			0 0				
			0 2 0	20.8	20.3	$Z=4$[d]	
			0 2 1	17.7	17.8		
			6 0 1	16.1	16.0		
			alkyl	4.2	–		
			π–π	3.3	–		
	RT	Col_{r2}	2 0 0	53.8	53.8	$a=107.6$	1.00
		P2gg	1 1 0	37.0	37.0	$b=39.4$	
			3 1	26.9	26.5, 26.9	$c=36.5$[c]	
			0, 4				
			0 0				
			4 1 1	19.0	19.0	$h=3.3$	
			2 2 1	16.5	16.5	$Z=4$[d]	
			4 2 1	14.4	14.6		
			1 3 0	13.3	13.0		
			alkyl	4.5 (br)	–		
			π–π	3.3	–		
	240[e]	Col_{r3}	2 0 0	33.4	33.6	$a=67.2$	0.88
		C2mm	1 1 0	31.7	31.7	$b=34.8$[c]	
			4 0 0	18.1	18.0	$Z=2$[d]	

[a] br = broad maximum.[b] Calculated density for two columns per unit cell in the case of Col_{r3} and 4 columns per unit cell in the cases of Col_{r1} and Col_{r2}. $\rho_{calcd}=(10\times Z\times M_r)/(a\times b\times h\times 6.02)$, in which M_r is the molecular weight and h is assumed to equal 3.3 Å for Col_{r3}. [c] c corresponds to the periodicity of the helix. [d] Z is the number of discotics per slice of the unit cell. [e] No WAXD measurement is available above 200 °C. [f] Crystalline phase.

rameters to those of the Col_r phase of the symmetrical parent compound when one takes into account the differences in the structure of the discotics and in the temperature of the measurements.[1] However, in Col_{r1} and Col_{r2} phases an unusual value of $Z=4$ was calculated based on density considerations (Table 2).[43] When comparing the lattice parameters, b is similar for all phases for both discotic **1** and discotic **2**, but a in Col_{r1} and Col_{r2} is nearly twice a in the Col_{r3}. It is assumed that at lower temperatures the symmetry decreases, and as a result two unit cells of Col_{r3} combined to give rise to the new unit cell of the Col_{r2} and Col_{r1} phases (Figure 4c). The loss of symmetry in the supramolecular organization when lowering the temperature might arise from different orientation in the plane of the nonsymmetric molecules or from a vertical shift of neighboring columns, which

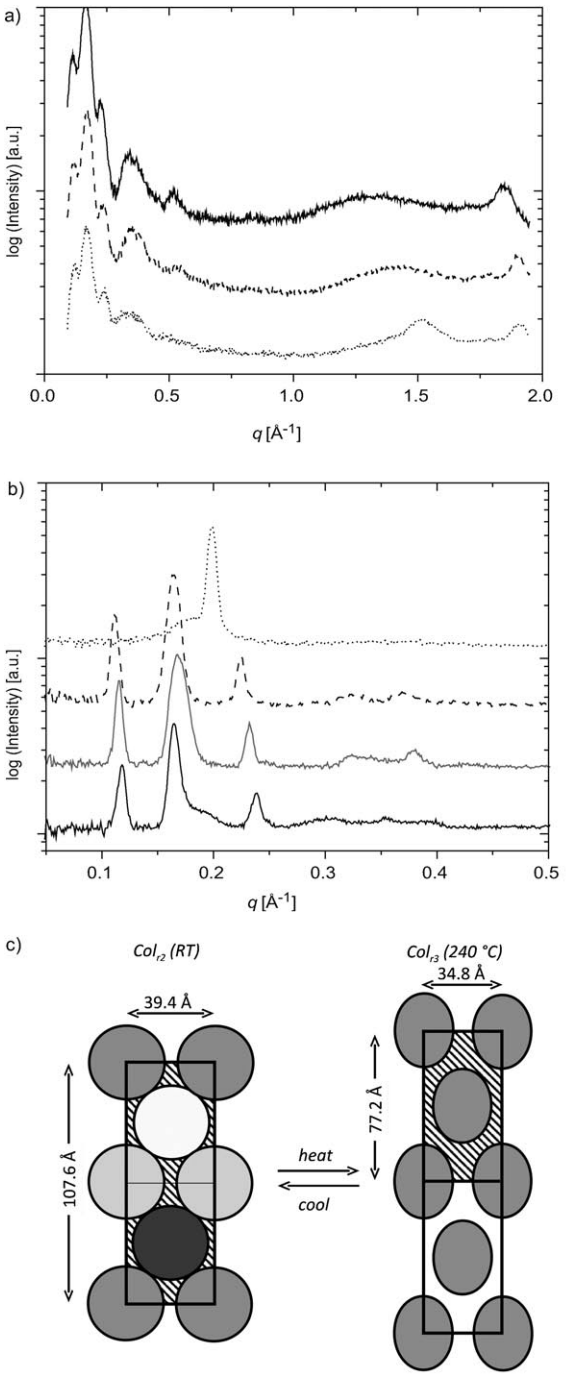

Figure 4. a) WAXD profiles for discotic **2** at −21 °C (•••••), RT (– – –), and 200 °C (——). b) SAXD profiles for discotic **2** at −21 °C (——), RT (——), 200 °C (– – –), and 240 °C (•••••). c) Proposed structures of Col_{r2} and Col_{r3} phases for discotic **2**. The unit cell is filled with diagonal lines. X-ray profiles of discotic **1** are given in Figure S4 of the Supporting Information.

are inherently helical, at least in solution as will be discussed below. X-ray diffraction studies on aligned samples can be used to elucidate the structure of the helix in the liquid-crystalline phase.[9,42,44] SAXD and WAXD patterns of an aligned sample of discotic **2** at RT (Col_{r2}) are shown in Figure 5. The meridional position of the peak due to the π–

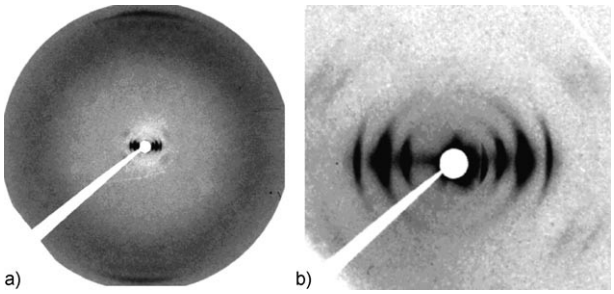

Figure 5. a) WAXD and b) SAXD patterns of an aligned sample of discotic **2** at RT. The capillary axis is vertical.

π stacking, in addition to the three most intense peaks in the small-angle region being on the equator, confirms that the phase is columnarly ordered with the central benzene ring of disc **2** being perpendicular to the axis of the columns (Figure 5a). In the helical organization, the molecules adopt a propeller shape in which the bipyridine units are tilted with respect to the central benzene unit (Figure 1b).[1] Therefore, an additional meridional maximum at a slightly lower diffraction angle than the π–π stacking maximum that corresponds to 3.7 Å is ascribed to the perpendicular distance between the bipyridine units of consecutive discs.[1] The less intense maxima in the small-angle region are split into a four-spot pattern (Figure 5b). This feature was ascribed to helical intracolumnar order and to the existence of three-dimensional order in the mesophase. From split maxima a periodicity of 36.5–38.0 Å can be measured along the axis of the columns. This value is only slightly larger than the periodicity in helices of the symmetrical analogue **A**,[1] although a value three times larger would be expected in this case due to the absence of C_3 symmetry. We have two hypotheses to explain this observation. Firstly, there is no correlation between the position of the pyridine moieties in consecutive discotics disordered along the column, so that the overall symmetry is the same as with C_3-symmetrical derivatives **A**.[1] Secondly, electron density is similar for the alkylated and nonalkylated wedges so that they are not distinguished by X-ray diffraction. In the structure we propose, the relative rotation between consecutive discotics in a column of discotic **2** is about 11° and around 33 discotics are needed for a complete rotation of 360°. A shift of the phase of neighboring columns/helices with a large correlation distance in the plane perpendicular to the columns could be the cause of the large size of the unit cell in the Col_{r1} and Col_{r2} phases. Upon an increase in the temperature, in Col_{r3} disorder increases and the correlation between the phases of neighboring columns is lost, thus resulting in an increase of the symmetry of the rectangular lattice.

Self-assembly and induction of chirality in solution: Besides the formation of columnar aggregates in the liquid-crystalline state, discotics **1** and **2** also self-assemble in nonpolar solution. Previous studies on C_3-symmetrical discotics based on the 3,3′-bis(acylamino)-2,2′-bipyridine units have revealed that they are preorganized by strong intramolecular hydrogen bonding between amide N−H and neighboring pyridine N atoms.[16] This hydrogen bonding was observed with ^{1}H NMR spectroscopy in $CDCl_3$ in which the amide protons were shifted downfield to approximately $\delta = 15$ ppm together with a downfield shift of several aromatic core protons, which is indicative of an on average almost flat shape of the discotic. This C_3-symmetrical preorganization allows the molecules to form long stacks primarily by π–π stacking, which leads to a propeller shape of the aggregated discotics inducing helicity, as is confirmed by X-ray diffraction (Figure 1b).[1] Since the helix is an intrinsically chiral object, chirality in the aliphatic periphery of the discotic is transferred to the helical stack. This process can be observed with circular dichroism (CD) spectroscopy by the appearance of a Cotton effect that corresponds to an electronic transition in UV/Vis absorption spectroscopy. First of all, ^{1}H NMR and CD spectroscopy of discotic **1** is discussed to prove that the conformation of discotic **1** in a good solvent ($CDCl_3$) and the self-assembly of discotic **1** in a nonsolvent (alkanes) are similar to that of C_3-symmetrical discotics in these solvents.[17] Secondly, the behavior of achiral discotic **2** has been probed with spectroscopic techniques to show that its behavior in solution is similar to that of discotic **1** and C_3-symmetrical analogues.

NMR spectroscopy: When an ^{1}H NMR spectrum of discotic **1** was taken in $CDCl_3$, protons characteristic of a preorganized structure were observed (Figure 6a). In chloroform, discotics **1** and **2** are mainly molecularly dissolved, thereby resulting in sharp peaks that allow for a structural investigation of the compounds. In a nonpolar solvent like heptane or methyl cyclohexane, molecules **1** and **2** are primarily stacked, which results in very broad NMR spectroscopic peaks. Peak assignment of discotics **1** and **2** in $CDCl_3$ was confirmed with gCOSY ^{1}H–^{1}H 2D NMR spectroscopy (see Figures S5 and S6 in the Supporting Information). Almost all aromatic and amide protons were observed in a 2:1 integration ratio that corresponds to the trialkoxyphenyl/phenyl wedge ratio of 2:1 (Figure 6). The secondary amide protons 7 are located between $\delta = 16$ and 14 ppm, indicative of very strong intramolecular hydrogen bonding with the nitrogen atoms of the bipyridine system. The aromatic protons 4 are located between $\delta = 9.6$ and 9.4 ppm due to strong anisotropic deshielding by the adjacent amide carbonyl. At $\delta = 9.25$ ppm, a singlet that belongs to central benzene core protons 10 and 11 is located. It is remarkable that protons 6′ and [6]′ of the outer pyridine rings are shifted $\delta = 0.6$ ppm downfield compared to protons 6 and [6] of the inner pyridine rings. This may reflect deshielding of protons 6′ and [6]′ by the neighboring amide carbonyls, which is a strong indication of an on average rather planar conformation of discotic **1**.[16] This means that the aromatic amide core of disc **1** is C_3 symmetrical as is drawn in Figure 6. Finally, between $\delta = 8.1$ and 7.2 ppm, less deshielded aromatic protons can be observed; their complete assignment is given in the Experimental Section. With an increase in the concentration of discotic **1** in $CDCl_3$, peak broadening and upfield shifts can be observed that are indicative of aggrega-

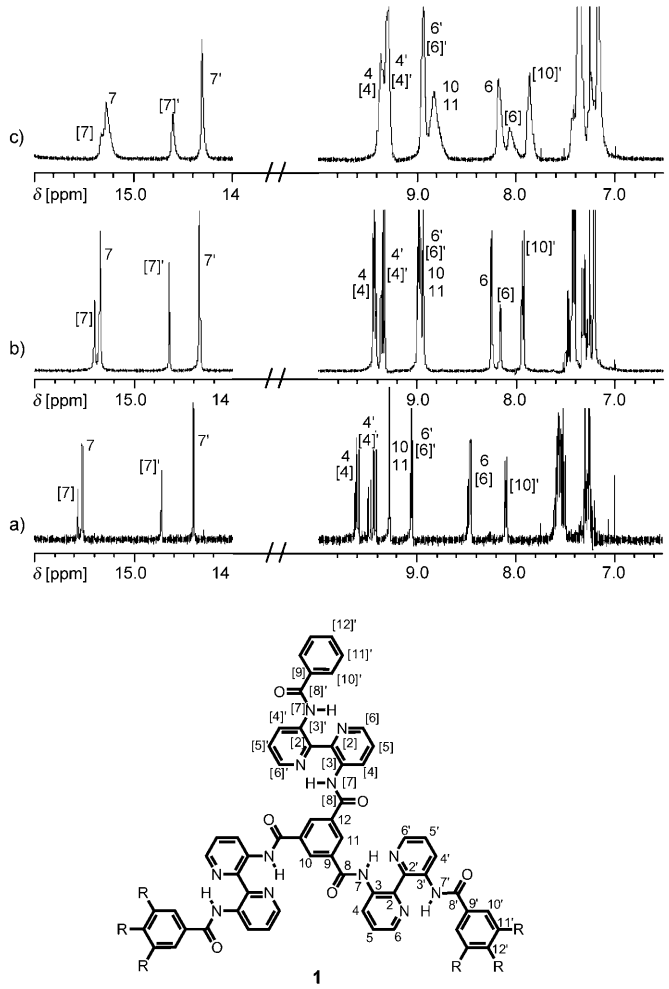

Figure 6. ^{1}H NMR spectra of discotic **1** in $CDCl_3$ at a) 0.5, b) 6, and c) 14 mM at 25 °C ($R = OC_{10}H_{21}$*). Only the aromatic and hydrogen-bonded proton region is shown. Full spectra are given in Figure S7 of the Supporting Information.

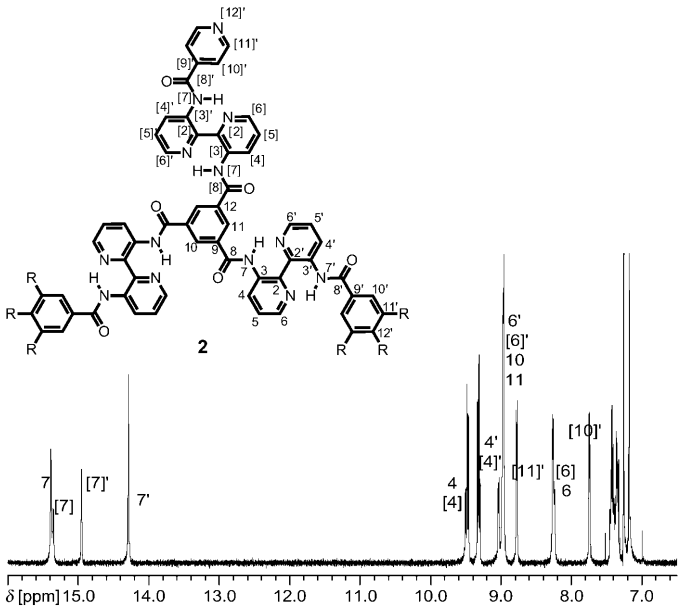

Figure 7. ^{1}H NMR spectra of discotic **2** in $CDCl_3$ at 3 mM. Only the hydrogen bonding and aromatic regions are shown. The full spectrum is given in Figure S8 of the Supporting Information ($R = OC_{12}H_{25}$).

tion (Figure 6b and c). In particular, the central phenyl protons 10 and 11 broaden and they also display the largest upfield shift ($\delta = 9.25$ to 8.8 ppm). However, no ordered, helical aggregates are formed in chloroform according to CD and UV/Vis spectroscopy. The observed ^{1}H NMR spectroscopic data of discotic **1** confirm that the conformation of disc **1** in chloroform is similar to that of its C_3-symmetrical derivatives. Thus, the removal of one alkylated group does not affect the overall conformation of discotic **1**.

The ^{1}H NMR spectrum of discotic **2** is depicted in Figure 7. It strongly resembles the spectrum of discotic **1** shown in Figure 6, which suggests that compounds **1** and **2** adopt a comparable conformation in solution. Also for discotic **2** separate aromatic and amide N–H peaks can be observed for the alkylated wedge and the nonalkylated wedge in an integration ratio of 2:1.

Optical spectroscopy: The self-assembly of discotic **1** was further investigated using CD spectroscopy with the goal of establishing how the removal of one alkylated, solubilizing group influences the self-assembly behavior of these discotics in nonpolar, dilute solution. To compare the aggregation behavior of discotic **1** with parent C_3-symmetrical compounds, a mixing experiment in which chiral discotic **1** was added to achiral, symmetric discotic **13** was performed (Figure 8).[17] C_3-symmetrical discotic **13** is known to self-assemble into well-defined supramolecular, helical columns in alkanes like heptane due to phase separation, π–π stacking, and preorganization by intramolecular hydrogen bonding. A chiral analogue of discotic **13** equipped with dihydro-citronellyl side chains (discotic **14**, Figure 8, right) is able to shift the equilibrium between right-handed (*P*) and left-handed (*M*) helices to one of them, thereby creating an overall chiral, supramolecular structure.[17] From mixing experiments in alkanes, it is known that a small amount of chiral discotic **14** is able to bias the helicity of columns of achiral discotic **13**. This is known as the "sergeant and soldiers" experiment in which chiral **14** acts as a sergeant directing a platoon of achiral discotic **13** soldiers.[20,45] If nonsymmetrical, chiral discotic **1** is able to bias the helicity of achiral discotic **13** in a similar fashion, and we may assume discotic **1** and achiral analogue **2** to display the same aggregation behavior as C_3-symmetrical discotic **13** and its analogues. The latter is a prerequisite to transfer the knowledge gained from symmetrical systems to the design of a nonsymmetrical discotic equipped with the desired functional group for supramolecular interactions. Thus, dilute solutions of discotic **1** in heptane were added to dilute solutions of discotic **13** of the same concentration in heptane (Figure 8). For every measuring point in Figure 8, a fresh mixture was prepared from the two stock solutions of discotics **1** and **13**, respectively.

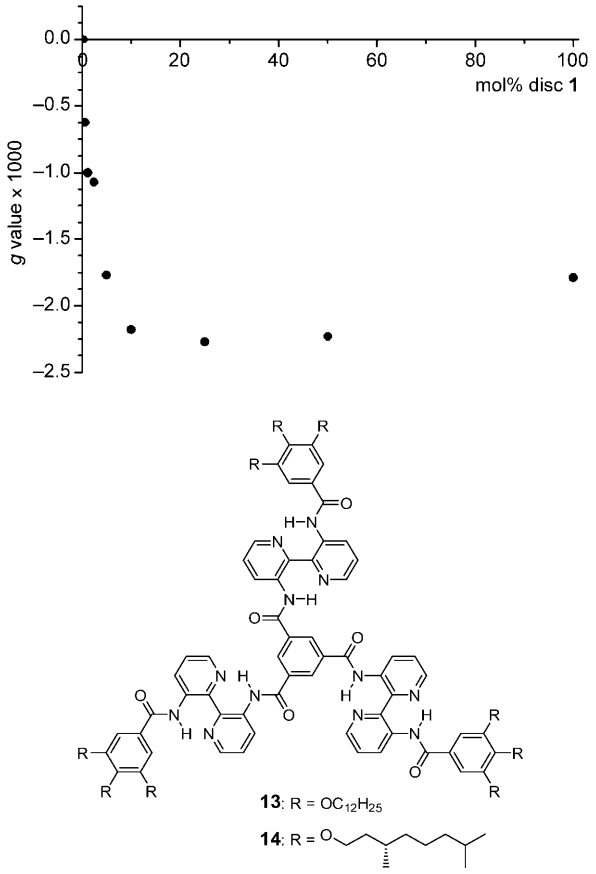

Figure 8. a) "Sergeant-and-soldiers" measurement with discotics **1** and **13**; the *g* values were measured at 387 nm for mixtures of discotics **1** and **13** in heptane at RT. Concentration = 27 μM. The magnitude of the Cotton effect is stable after mixing. Full CD and UV/Vis spectra are given in Figure S9 of the Supporting Information. b) C_3-symmetrical discotics achiral **13** and chiral **14**.

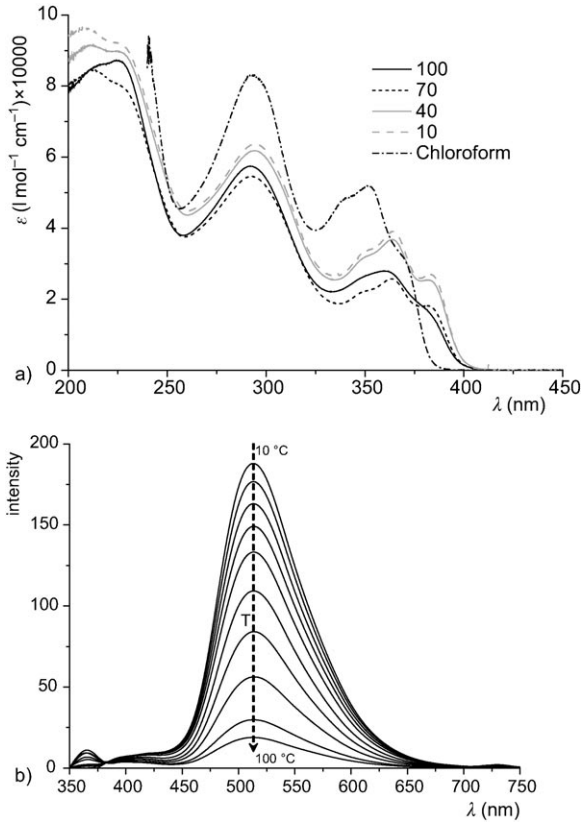

Figure 9. a) Temperature-dependent UV/Vis absorption spectra of discotic **2** in dodecane;[49] $c = 17$ μM, cooling rate = 1 K min^{-1}. The spectrum in chloroform was taken at RT, $c = 19$ μM (full temperature ranges are given in Figure S10 of the Supporting Information). b) Temperature-dependent fluorescence spectra of discotic **2** in dodecane; $c = 1$ μM, cooling rate = 1 K min^{-1}. Excitation performed at 365 nm.

In Figure 8a, the Cotton effect, given as the anisotropic *g* factor, is plotted against the amount of chiral disc **1** added; a strong nonlinear dependence is clearly visible. After the addition of just 5 mol% chiral disc **1**, the same amplitude of the Cotton effect as with 100 mol% chiral **1** was observed. This indicates a strong bias of the helical sense of assemblies of achiral **13** by chiral **1**, thus strongly suggesting the presence of mixed assemblies of discotic **1** with **13**. The Cotton effect emerged immediately after mixing and was stable with time, thereby indicating that the dynamic system immediately adopts its thermodynamically most favorable state. The maximum in CD intensity was observed around 25 mol% disc **1**, which might be rationalized by more efficient packing of achiral disc **13**, which lacks methyl branches, relative to chiral disc **1**. A dependence of the aggregation on the branched character of the aliphatic periphery has been observed for hexabenzocoronene discotics.[46]

For achiral discotic **2**, temperature-dependent self-assembly in nonpolar solution has been examined with UV/Vis and fluorescence spectroscopy to study its aggregation behavior in diluted nonpolar solution (Figure 9). Upon cooling, the UV/Vis absorption spectrum of discotic **2** in dodecane displayed a bathochromic and hypsochromic shift between 100 and 70 °C, and a bathochromic and hypsochromic shift between 70 and 10 °C (Figure 9a). The bathochromic shift of the absorption maximum belonging to the gallic moieties amounts to 2 nm (292–294 nm), and the bathochromic shift of the absorption maximum belonging to the bipyridine moiety amounted to 4 nm (360–364 nm). In the region of the π–π* transition of the bipyridine system around 362 nm, the fine structure was observed in a more pronounced fashion. This fine structure, with absorption maxima at 364 and 383 nm and a shoulder at 351 nm, is indicative of the formation of well-ordered, helical stacks in solution. The shape of the spectrum at 100 °C is similar to a spectrum of discotic **2** in chloroform (Figure 8), in which the discotics are molecularly dissolved. The latter spectrum shows a hypsochromic shift of about 12 nm compared to the spectrum of discotic **2** in dodecane. In the fluorescence spectrum (Figure 9b), a large, gradual increase of the fluorescence intensity can be observed upon cooling. This increase is, together with the redshift in UV/Vis, indicative of the formation of J-aggregates in dilute solutions in dodecane, a phenomenon also observed for discotics that contain oxadiazole moieties.[47] This formation of J-aggregates coincides with our molecular picture of a helical stack of discotic **2** in

which the 3,3′-bis(acylamino)-2,2′-bipyridine chromophores are placed on top of each other in a slipped and tilted ship-screw-like manner (Figure 1b).[1,17] When a dilute solution of discotic **2** in dodecane was heated to 100 °C, the fluorescence was largely quenched as in a solution of **2** in chloroform at room temperature in which the molecularly dissolved state of **2** is present. The fluorescence maximum is located at 513 nm, thus reflecting a large Stokes shift of about 148 nm, presumably due to intramolecular double-proton transfer within the diamino bipyridine moieties in the excited state.[48]

Conclusion

Nonsymmetrical discotics **1** and **2** based on 2,2′-bipyridine-3,3′-diamine units linked to a trimesic core have been successfully synthesized and characterized. These mesogens display columnar liquid crystallinity over a very broad temperature window (>300 K) in which two different rectangular columnar mesophases are observed. The columns in the mesophase possess a helical structure with a small relative rotation of about 11° between superimposed molecules, similar to their C_3-symmetrical analogues. In solution, NMR spectroscopic measurements on discotics **1** and **2** revealed an on average rather flat conformation when they are in the molecular dissolved state. The aromatic amide core of the discs is C_3 symmetrical in this conformation. Optical spectroscopy showed well-ordered helical stacking in nonsolvents like alkanes together with expression and amplification of chirality as is observed for disc **1** with a "sergeant and soldiers" mixing experiment. Excitingly, the replacement of one of the trialkoxyphenyl disordered wedges by a aromatic, rigid wedge does not prevent the formation of columnar liquid-crystalline phases and highly ordered helical stacking in solution. They even mix at the molecular level with their C_3-symmetrical parent compounds. This might enable functionalization of molecules like **2** with the goal of introducing catalytic sites or functionality by secondary interactions.

Experimental Section

General: ^{1}H and ^{13}C NMR spectra were recorded using a Varian Mercury Vx 400 MHz (100 for ^{13}C), a Varian Gemini 300 MHz (75 MHz for ^{13}C), or a Varian Mercury Plus 200 MHz (50 MHz for ^{13}C) NMR spectrometer. ^{1}H chemical shifts were determined with tetramethylsilane as internal standard ($\delta = 0$ ppm). ^{13}C chemical shifts were determined from the deuterated solvent $CDCl_3$ ($\delta = 77.36$ ppm) or tetramethylsilane ($\delta = 0$ ppm) as internal standard. gCOSY 2D experiments were performed in $CDCl_3$ using a Varian Mercury 400 MHz spectrometer with standard Varian parameters for $CDCl_3$. CD spectra were recorded using a Jasco J-600 spectropolarimeter equipped with a Jasco PTC-348WI Peltier-type temperature control system, UV/Vis spectra were recorded using a Perkin–Elmer Lambda 40 UV/Vis spectrometer equipped with a Perkin–Elmer PTP-1 Peltier temperature control system, and fluorescence spectra were measured using a Perkin–Elmer LS50B luminescence spectrometer equipped with a Perkin–Elmer PTP-1 Peltier temperature control system. A 1 cm quartz cuvette was used for the measurements, wavelengths are given in nm, and absorptions in $L\,mol^{-1}\,cm^{-1}$. Thermal gravimetric analysis (TGA) was carried out on a Perkin–Elmer Pyris 6 Thermogravimetric Analyzer. Heating was performed from 30 to 600 °C with a slope of 10 °C min^{-1} under a nitrogen atmosphere. Polarized optical microscope images were made using a Carl Zeiss Jenaval polarization microscope equipped with a Linkam THMS 600 heating device and a Polaroid digital camera model PDMC-2. Measurements were performed under a nitrogen atmosphere to prevent thermal degradation. DSC analysis was performed using a Perkin–Elmer Pyris 1 or Thermal Analysis Q2000 instrument under a nitrogen atmosphere. For all SAXD and WAXD measurements, the crude product was filled in a Lindemann glass capillary (0.9 mm diameter). Aligned samples were obtained by shearing inside the capillary at the temperature of the mesophase, typically at 160 °C. The studies on the aligned sample were carried out at University of Zaragoza with a pinhole camera (Anton Paar) operating with a point-focused Ni-filtered Cu_{Ka} beam. The capillary axis was perpendicular to the X-ray beam, and the pattern was collected on a flat photographic film perpendicular to the beam. Spacings were obtained by means of Bragg's law. In this setup, the whole beam path was under vacuum for RT measurements. SAXD measurements were made using a homemade setup with a rotating anode X-ray generator (Rigaku RU-H300, 18 kW) equipped with two parabolic multilayer mirrors (Bruker, Karlsruhe, Germany), thereby giving a highly parallel beam (divergence about 0.025°) of monochromatic Cu_{Ka} radiation, ($\lambda = 1.54$ Å). The SAXD intensity was collected with a two-dimensional gas-filled wire detector (Bruker Hi-Star). To change the temperature, an adapted Linkam THMS 600 hot stage was used. Powder WAXD measurements were performed using a home-built system at Philips (Eindhoven) consisting of a sealed X-ray tube (Cu_{Ka} radiation), a primary graphite monochromator, a pinhole collimator, a sample stage, and a Siemens Hi-Star area detector. Samples were prepared in a 0.9 mm diameter Lindemann capillary tube and mounted in a home-built furnace based on a TMS94 Linkam hot stage. WAXD patterns were recorded with a sample-to-detector distance of 8.1 cm.

Please see the Supporting Information for further Experimental details.

3′-Benzoylamino-2,2′-bipyridine-3-amine (4):[15] Under argon, a solution of benzoyl chloride (0.88 mL, 10.2 mmol) in dry diethyl ether (110 mL) was added dropwise to an ice-cold well-stirred dark yellow suspension of **3**[50] (1.744 g, 9.37 mmol) and triethylamine (1.65 mL, 11.9 mmol) in distilled diethyl ether (95 mL). After 15 min, a white-yellow precipitate formed and the solution turned brownish. The reaction mixture was allowed to reach RT and stirred for 28 h under argon. Subsequently, the brown-yellow suspension was washed with ice-cold water (2×100 mL), the aqueous layers were combined and extracted with dichloromethane (2×50 mL). The organic layers were combined, after which a clear brown solution was obtained. This organic layer was washed with brine (2×100 mL), dried with $MgSO_4$, and filtered. Concentration of the filtrate in vacuo gave a brownish residue that was purified by column chromatography (silica gel, 3 vol% CH_3CN in $CHCl_3$ to elute the bisamide side product and 10 vol% CH_3CN in $CHCl_3$ to elute the target product), which gave amine **4** as a yellow powder. Finally, recrystallization from boiling CH_3CN (30 mL) gave pure title product **4** (2.35 g, 85%) as a crystalline, yellow compound. $R_f = 0.29$ (silica gel, 3 vol% CH_3CN in $CHCl_3$); GC–MS: $t_R = 8.26$ min; m/z: calcd: 290.12; found: 290 (radical cation); m.p. 168.0–168.5 °C (lit. 167.5–168.5 °C); ^{1}H NMR (400 MHz, $CDCl_3$, 25 °C): $\delta = 14.70$ (s, 1H; [7]′), 9.29 (d, $^3J(H,H) = 8.46$ Hz, 1H; [4]′), 8.31 (d, $^3J(H,H) = 4.43$ Hz, 1H; [6]′), 8.07 (d, $^3J(H,H) = 6.25$ Hz, 2H; [10]′), 8.00 (m, 1H; [6]), 7.56–7.49 (3H; [11]′+[12]′), 7.30 (dd, $^3J(H,H) = 8.46$ and 4.43 Hz, 1H; [5]′), 7.13–7.08 (2H; [4]+[5]), 6.60 ppm (s, 2H; [7]); ^{13}C NMR (100 MHz, $CDCl_3$, 25 °C, APT): $\delta = 166.6$, 145.3, 143.7, 140.9, 138.6, 136.4, 135.8, 134.9, 131.8, 128.7, 128.6, 127.6, 125.4, 124.2, 122.8 ppm; FTIR (ATR): $\tilde{\nu} = 3427$ (NH_2), 3285 (NH_2), 3028, 2754 (C–H aryl), 1649 (amide C=O), 1601, 1569 (amide N–H), 1558, 1520, 1492, 1471, 1453, 1429, 1397, 1323, 1309 (amide C–N), 1272, 1250, 1208, 1198, 1162, 1066, 1028, 1001, 979, 967, 930, 906, 865, 795, 733, 720, 701, 672 ppm; elemental analysis calcd (%) for $C_{17}H_{14}N_4O$: C 70.33, H 4.86, N 19.30; found: C 70.04, H 4.76, N 19.17.

3′-*tert*-Butoxycarbonylamino-2,2′-bipyridine-3-amine (5): Under argon, 2,2′-bipyridine-3,3′-diamine (**3**) (3.310 g, 17.78 mmol) and di-*tert*-butyl dicarbonate (4.646 g, 21.29 mmol) were dissolved in ethanol (32 mL) at RT while being stirred. The stirred solution was heated at 35 °C for 5.5 h, allowed to reach RT, and then diethyl ether (100 mL) was added. The obtained orange solution was washed with dilute brine (3×50 mL), dried with $MgSO_4$, and filtered. Concentration of the filtrate in vacuo gave an orange, sticky residue that was purified by column chromatography (silica gel, 20 vol% ethyl acetate in heptane to elute the di-Boc-protected side product and 40 vol% ethyl acetate in heptane to elute the desired compound) to give **5** as a yellow, thick syrup that solidified after thorough drying (3.378 g, 73%). R_f=0.39 (silica gel, 40 vol% ethyl acetate in $CHCl_3$); GC–MS: t_R=6.51 min; *m/z*: calcd: 286.34; found: 286 (radical cation); m.p. 83.0–84.5 °C; ^{1}H NMR (400 MHz, $CDCl_3$, 25 °C): δ=12.46 (s, 1H; 7′), 8.75 (d, ^3J(H,H)=8.43 Hz, 1H; 4′), 8.21 (d, ^3J(H,H)=4.40 Hz, 1H; 6′), 7.99 (d, ^3J(H,H)=3.66 Hz, 1H; 6), 7.21 (dd, ^3J(H,H)=8.43, 4.40 Hz, 1H; 5′), 7.06–7.04 (2H; 4+5), 6.36 (s, 2H; 7), 1.53 ppm (s, 9H; 11′); ^{13}C NMR (75 MHz, $CDCl_3$, 25 °C, APT): δ=153.5, 144.6, 143.1, 139.6, 138.8, 136.3, 135.3, 127.2, 124.8, 123.8, 122.6, 80.0, 28.4 ppm; FTIR (ATR): $\tilde{\nu}$=3429 (NH_2), 3291 (NH_2), 3055, 2980, 2928 (C−H aryl and alkyl), 1700 (urethane C=O), 1604, 1578 (urethane N−H), 1504, 1475, 1454, 1438, 1402, 1391, 1366, 1330, 1308, 1297, 1273, 1247, 1212, 1196, 1157, 1124, 1079, 1067, 1050, 1025, 972, 932, 906, 866, 835, 790, 775, 748, 731, 701 cm^{-1}; elemental analysis calcd (%) for $C_{15}H_{18}N_4O_2$: C 62.92, H 6.34, N 19.57; found: C 62.77, H 6.28, N 19.54.

***N*-{3[3′-(Benzoylamino)-2,2′-bipyridyl]}-*N*′,*N*″-bis{3[3′-(*tert*-butoxycarbonylamino)-2,2′-bipyridyl]}benzene-1,3,5-tricarboxamide (6)**: Under argon, diisopropylethylamine (0.70 mL, 4.0 mmol) and aromatic amine **4** (0.984 g, 3.39 mmol) dissolved in distilled dichloromethane (60 mL) were added dropwise to a well-stirred, chilled (10 °C) solution of trimesyl chloride (0.90 g, 3.39 mmol) in distilled dichloromethane (60 mL). After 3 h of being stirred while the reaction temperature was allowed to reach RT, diisopropylethylamine (1.4 mL, 2.092 g) and aromatic amine **5** (2.092 g, 7.306 mmol) dissolved in distilled dichloromethane (55 mL) were added dropwise to the well-stirred, chilled (10 °C) white suspension. The yellow, clear solution was stirred under argon overnight after which a dark orange reaction mixture containing a white precipitate was obtained that was concentrated in vacuo. The residue was dissolved in a minimal amount of hot chloroform (12 mL) and precipitated in chilled methanol (160 mL). Filtration over a Büchner funnel yielded a beige residue which was washed with methanol (2×20 mL), redissolved in chloroform (150 mL) and filtered over celite. Concentration of the filtrate in vacuo yielded a beige residue that was purified by column chromatography (silica, 3 vol% pyridine in chloroform) to give discotic **6** as a beige, sticky solid (2.140 g, 62%) that was used as such. R_f=0.32 (silica gel, 4 vol% pyridine in $CHCl_3$); t_R=14.48 min (analytical GPC, $CHCl_3$, 2×PL gel 3 mm 100 Å column, one peak); decomposes; ^{1}H NMR (400 MHz, $CDCl_3$, 25 °C): δ=14.41 (s, 1H; [7]), 14.38 (s, 2H; 7), 14.27 (s, 1H; [7]′), 12.65 (s, 2H; 7′), 8.81 (d, ^3J(H,H)=7.42 Hz, 1H; [4]), 8.53 (d, ^3J(H,H)=7.43 Hz, 1H; [4]′), 8.44–8.42 (m, 4H; 4+4′), 8.36 (d, ^3J(H,H)=2.74 Hz, 1H; [6]′), 8.33 (d, ^3J(H,H)=2.74, 1H; 6′), 7.84 (s, 1H; 10), 7.73 (s, 2H; 11), 7.63 (d, ^3J(H,H)=6.64 Hz, 2H; [10]′), 7.50 (d, ^3J(H,H)=2.74 Hz, 2H; 6), 7.37 (t, ^3J(H,H)=6.64 Hz, 1H; [12]′), 7.32–7.26 (m, 3H; [6] and [11]′), 6.88 (dd, ^3J(H,H)=7.82, 3.52 Hz, 2H; 5), 6.81 (dd, ^3J(H,H)=7.82, 3.52 Hz, 1H; [5]), 6.46 (dd, ^3J(H,H)=7.42, 3.52 Hz, 2H; 5′), 6.41 (dd, ^3J(H,H)=7.42, 3.52 Hz, 1H; [5]′), 1.49 ppm (s, 18H; 11′); FTIR (ATR): $\tilde{\nu}$=2953 (C−H alkyl), 2925 (C−H alkyl), 2869 (C−H alkyl), 1670 (amide C=O), 1567 (amide N−H), 1509 (aromatic), 1492 (aromatic), 1468, 1445, 1427, 1369, 1328, 1296 (amide C−N), 1239, 1201, 1115, 1074, 1045, 1029, 997, 945, 913, 865, 798, 746, 730, 716, 700 cm^{-1}; MALDI-TOF MS: *m/z*: calcd: 1018.39; found: 1019.27 [*M*+H$^+$], 1041.27 [*M*+Na$^+$], 1057.27 [*M*+K$^+$].

3,4,5-Tris-((*S*)-3,7-dimethyloctyloxy)benzoyl chloride (9): Under argon, thionyl chloride (3.5 mL, 29.4 mmol) and DMF (2 drops) were added at RT to a stirred solution of benzoic acid **8** (0.534 g, 0.903 mmol) in distilled dichloromethane (20 mL). The reaction mixture was stirred overnight at RT, concentrated in vacuo, and placed under high vacuum to remove all traces of volatile compounds to yield a beige, thick oil that was used as such. FTIR (ATR): $\tilde{\nu}$=3433, 2954, 2926, 2870, 1752 (C=O), 1581, 1496, 1466, 1428, 1383, 1366, 1324, 1235, 1185, 1140, 1115, 1028, 984, 918, 852, 762, 736, 693, 665 cm^{-1}.

***N*,*N*′-Bis{3[3′-(3,4,5-tris((*S*)-3,7-dimethyloctyloxy)benzoylamino)-2,2′-bipyridyl]}-*N*″-{3[3′-(benzoylamino)-2,2′-dipyridyl]}benzene-1,3,5-tricarboxamide (1)**: Under argon, a mixture of TFA and dichloromethane (10 mL, 1:1 v/v) was added dropwise to an ice-cold stirred solution of **6** (0.806 g, 0.791 mmol) in distilled dichloromethane (20 mL). The yellow reaction mixture was stirred at RT for 5 h, concentrated in vacuo without heating,[51] and dried under vacuum to yield a dark yellow shining residue, which was subsequently dissolved in acetone (30 mL). Triethylamine (5 mL) dissolved in acetone (25 mL) was added dropwise to this stirred solution of the TFA salt, after which the obtained beige suspension was stirred for another 10 min and filtered over a Büchner funnel. The residue was washed with acetone (2×10 mL) and ethanol (2×50 mL) to yield yellowish product **7** (0.5274 g, 81%) that was used as such.

Under argon, diamine **7** (0.333 g, 0.406 mmol), gallic acid chloride **9** (0.550 g, 0.903 mmol), and diisopropylethylamine (0.3 mL, 1.72 mmol) were mixed in distilled *N*-methyl-2-pyrrolidone (5 mL) at RT and stirred overnight. The obtained thick, yellow suspension was concentrated in vacuo, dissolved in hot $CHCl_3$ (5 mL), and subsequently suspended in ice-cold methanol (150 mL). The beige suspension was filtered using a Büchner funnel yielding a beige residue (0.703 g), which was washed with methanol (2×25 mL). The beige residue was purified by column chromatography (flash silica, 4 vol% ethyl acetate in chloroform to elute a less-polar side product, 5 vol% ethyl acetate in chloroform to elute the desired product) to yield the desired title compound **1** (0.173 g, 22%) as a beige, sticky compound. R_f=0.32 (silica gel, 4 vol% ethyl acetate in $CHCl_3$); t_R=12.2 min (analytical GPC, $CHCl_3$, 2×PL gel 3 mm 100 Å column, one peak); ^{1}H NMR (400 MHz, $CDCl_3$, 25 °C, 6 mM): δ=15.40 (s, 1H; [7]), 15.35 (s, 2H; 7), 14.65 (s, 1H; [7]′), 14.34 (s, 2H; 7′), 9.45–9.41 (3H; 4+[4]), 9.36–9.32 (3H; 4′+[4]′), 9.00–8.96 (4H; 6′+[6]′+10), 8.94 (s, 2H; 11), 8.25 (d, ^3J(H,H)=4.4 Hz, 2H; 6), 8.16 (d, ^3J(H,H)=3.07 Hz, 1H; [6]), 7.93 (d, ^3J(H,H)=7.04 Hz, 2H; [10]′), 7.48–7.46 (m, 1H; [12]′), 7.44–7.40 (5H; 5′+[5]′+[11]′), 7.32 (dd, ^3J(H,H)=8.14, 4.40 Hz, 2H; 5), 7.27 (dd, ^3J(H,H)=8.36, 4.40 Hz, 1H; [5]), 7.21 (s, 4H; 10′), 4.11–4.03 (12H; 13′+14′), 1.95–1.86 (m, 6H; 15′), 1.76–1.74 (m, 12H; 16′), 1.69–1.53 (18H; 15′+17′+20′), 1.34–1.16 (30H; 17′+18′+19′), 1.00–0.94 (m, 18H; 22′), 0.90 ppm (d, ^3J(H,H)=6.60 Hz, 36H; 21′); ^{13}C NMR (400 MHz, $CDCl_3$ with 8 vol% hexafluoroisopropanol (HFIP) 25 °C, 6 mM): δ=167.5, 167.4, 164.0, 163.9, 153.3, 142.1, 142.0, 141.7, 141.5, 141.4, 140.4, 137.4, 137.2, 136.9, 136.8, 136.7, 135.7, 135.6, 134.6, 134.5, 132.5, 130.0, 129.9, 129.4, 128.9, 127.3, 124.7, 124.2, 106.4, 72.6, 68.1, 39.5, 39.4, 37.6, 37.5, 37.3, 36.5, 30.0, 29.9, 28.1, 24.9, 24.8, 22.8, 22.7, 22.6, 19.6, 19.5 ppm; FTIR (ATR): $\tilde{\nu}$=2953 (C−H alkyl), 2925 (C−H alkyl), 2869 (C−H alkyl), 1670 (amide C=O), 1567 (amide N−H), 1509 (aromatic), 1492 (aromatic), 1468, 1445, 1427, 1369, 1328, 1296 (amide C−N), 1239, 1201, 1115, 1074, 1045, 1029, 997, 945, 913, 865, 798, 746, 730, 716, 700 cm^{-1}; UV/Vis (heptane, 27 mM, 25 °C): λ_{max} (ε)=209 (63.3×10^3), 291 (40.8×10^3), 351 (shoulder, 14.6×10^3), 364 (18.2×10^3), 383 nm (13.8×10^3 M^{-1}cm^{-1}); UV/Vis (chloroform, 36 mM, 25 °C): λ_{max} (ε)=292 (83.0×10^3), 341 (shoulder, 47.7×10^3), 352 (51.1×10^3), 368 nm (shoulder, 32.6×10^3 M^{-1}cm^{-1}); MALDI-TOF MS: *m/z*: calcd: 1964.25; found: 1965.26 [*M*+H$^+$], 1987.23 [*M*+Na$^+$], 2003.24 [*M*+K$^+$], 2028.18 [*M*+Cu$^+$]; elemental analysis calcd (%) for $C_{120}H_{162}N_{12}O_{12}$: C 73.36, H 8.31, N 8.56; found: C 73.47, H 8.56, N 8.45.

Pyridine-4-carbonyl chloride·HCl (10): Under argon, isonicotinic acid (2.059 g, 16.7 mmol) was added slowly to stirred thionyl chloride (80 mL) heated at reflux. The reaction mixture was heated at reflux for 5 h and subsequently concentrated in vacuo, thus yielding a beige solid. High vacuum was used to remove traces of volatile compounds. The residue was used without further purification. ^{1}H NMR (200 MHz, [D$_6$]acetone, 25 °C): δ=9.43 (d, 2H; [10]′), 8.84 ppm (d, 2H; [11]′); FTIR (ATR): $\tilde{\nu}$=3070, 2965, 2714, 2563, 2097, 2016, 1892, 1814, 1750, 1732, 1637, 1607, 1506, 1497, 1394, 1336, 1275, 1236, 1195, 1129, 1064, 1044, 1003, 898, 823, 757, 729, 684 cm^{-1}.

3′-(4-Pyridylcarbonylamino)-2,2′-bipyridine-3-amine (11): Under argon, HCl salt **10** (2.97 g, 16.7 mmol) dissolved in distilled dichloromethane (110 mL) and DIPEA (4 mL) was added dropwise to a well-stirred, ice-

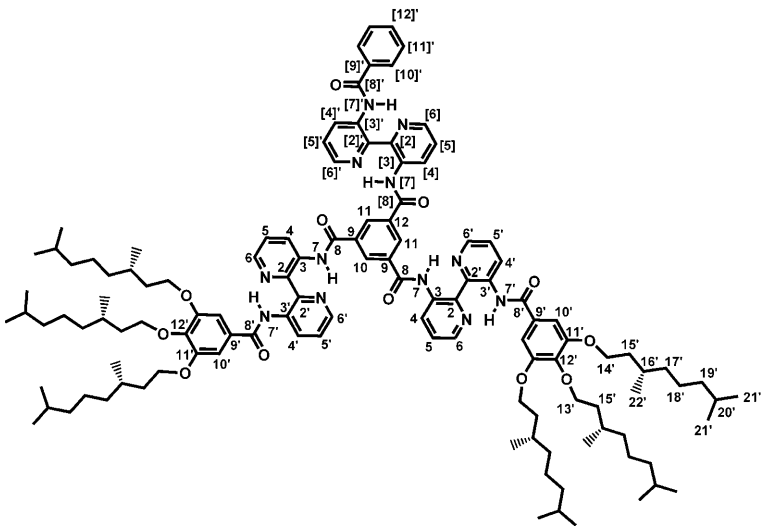

cold solution of **3** (2.590 g, 13.9 mmol) and DIPEA (3 mL) in distilled dichloromethane (110 mL). The stirred, brownish, clear reaction mixture was allowed to reach RT and stirred for an additional 5 h, after which the reaction mixture was washed with aqueous Na_2CO_3 solution (saturated, 2×50 mL). The aqueous layers were combined and extracted with dichloromethane (1×50 mL). The combined organic layers were washed with brine (2×25 mL) and dried with $MgSO_4$. Filtration gave a clear, brown solution that was concentrated in vacuo. Column chromatography (silica, 5 vol% pyridine in chloroform) of the residue yielded a yellow compound that was crystallized from a mixture of boiling ethanol (200 mL) and ethyl acetate (5 mL) to yield product **11** as yellow needles (2.02 g, 50%). R_f=0.33 (silica gel, 5 vol% pyridine in $CHCl_3$); GC–MS: t_R=9.15 min; *m/z*: calcd: 291.11; found: 291 (radical cation); m.p. 199.5–200.0 °C; ^{1}H NMR (400 MHz, $CDCl_3$, 25 °C): δ=15.10 (s, 1H; [7]′), 9.25 (d, ^3J(H,H)=8.30 Hz, 1H; [4]′), 8.84 (d, ^3J(H,H)=4.57 Hz, 2H; [11]′), 8.36 (d, ^3J(H,H)=4.57 Hz, 1H; [6]′), 8.00 (d, ^3J(H,H)=3.95 Hz, 1H; [6]), 7.89 (d, ^3J(H,H)=4.57 Hz, 2H; [10]′), 7.32 (dd, ^3J(H,H)=8.30, 4.57 Hz, 1H; [5]′), 7.18–7.12 (2H; [4]+[5]), 6.70 ppm (s, 2H; [7]); ^{13}C NMR (50 MHz, $CDCl_3$, 25 °C, APT): δ=164.1, 150.7, 145.4, 143.6, 142.8, 141.3, 138.0, 135.7, 134.6, 128.5, 125.5, 124.4, 122.6, 121.2 ppm; FTIR (ATR): $\tilde{\nu}$=3357 (NH_2), 3241 (NH_2), 3026, 2821 (C–H aryl), 1946, 1664 (amide C=O), 1605, 1572 (amide N–H), 1554, 1512, 1493, 1473, 1454, 1439, 1408, 1400, 1346, 1327, 1312, (amide C–N), 1276, 1259, 1216, 1200, 1152, 1132, 1099, 1060, 999, 972, 959, 910, 875, 847, 819, 797, 750, 732, 721, 696, 674 cm^{-1}; elemental analysis calcd (%) for $C_{16}H_{13}N_5O$: C 65.97, H 4.50, N 24.04; found: C 65.57, H 4.22, N 23.70.

***N*-{3[3′-(4-Pyridyl-carbonylamino)-2,2′-bipyridyl]}-*N*′,*N*″-bis{3[3′-(3,4,5-tris(dodecyloxy)benzoylamino)-2,2′-bipyridyl]}benzene-1,3,5-tricarboxamide (2)**: Under argon, a mixture of aromatic monoamine **11** (0.759 g, 2.60 mmol) and DIPEA (0.9 mL) mixed in distilled dichloromethane (65 mL) was added to a chilled, well-stirred solution of trimesyl chloride (0.693 g, 2.61 mmol) in distilled dichloromethane (65 mL). After 10 min, a solution of nonpolar monoamine **12** (4.600 g, 5.45 mmol) and DIPEA (1.2 mL) in distilled dichloromethane (5 mL) was added slowly to the brownish, turbid, well-stirred reaction mixture. The reaction mixture was stirred for another 3 h and subsequently concentrated in vacuo. The obtained dark gray residue was dissolved in hot chloroform (20 mL) and precipitated dropwise in acetone (250 mL) while stirring. Then the suspension was filtered using a Büchner funnel. The gray residue was dissolved in hot chloroform (50 mL) and mixed with acetone (100 mL) to obtain a gray suspension that was heated at reflux for 0.5 h and filtered on a Büchner funnel to yield a gray residue that was washed with a mixture of acetone and chloroform (10 vol% chloroform in acetone, 2×20 mL). Repetitive column chromatography (silica gel, 2 vol% ethyl acetate in chloroform; silica gel, 2.5 vol% methanol in chloroform; and flash silica gel, 5–10 vol% triethyl amine in chloroform) gave after evaporation of the product fractions a crude, brown-beige product (0.886 g, 16%). Finally, 0.290 g crude product was purified using preparative recycling GPC (chloroform, 2×Jai-Gel column) to yield desired discotic **2** (0.224 g, 77%) as a beige-white sticky solid. R_f=0.34 (silica gel, 5 vol% triethyl amine in $CHCl_3$), t_R=12.1 min (GPC, $CHCl_3$, 2×PL gel 3 mm 100 Å column, one peak); ^{1}H NMR (400 MHz, $CDCl_3$, 25 °C, 3.3 mM): δ=15.39 (s, 2H; 7), 15.36 (s, 1H; [7]), 14.96 (s, 1H; [7]′), 14.29 (s, 2H; 7′), 9.50–9.46 (3H; 4+[4]), 9.33–9.30 (3H; 4′+[4]′), 9.03 (d, ^3J(H,H)=6.28 Hz, 1H; [6]′), 8.97–8.96 (5H; 10+11+6′), 8.78 (d, ^3J(H,H)=6.04 Hz, 2H; [11]′), 8.27–8.24 (3H; 6+[6]), 7.75 (d, ^3J(H,H)=5.64 Hz, 2H; [10]′), 7.46–7.39 (3H; 5′+[5]′), 7.38–7.33 (3H; 5+[5]), 7.18 (s, 4H; 10′), 4.05–4.00 (12H; 13′+14′), 1.89–1.75 (12H; 15′), 1.53–1.48 (12H; 16′), 1.39–1.29 (96H; 17′), 0.92–0.87 ppm (18H; 18′); ^{13}C NMR (400 MHz, $CDCl_3$ with 8 vol% HFIP, 25 °C, 28 mM): δ=168.5, 165.3, 165.2, 165.1, 153.5, 149.4, 144.2, 143.0, 142.8, 142.3, 142.3, 141.6, 141.5, 141.1, 137.3, 137.0, 136.8, 136.5, 136.4, 131.1, 131.0, 130.8, 130.7, 130.5, 130.1, 125.2, 125.1, 125.0, 124.8, 122.4, 106.4, 75.0, 70.0, 32.2, 32.2, 30.2, 30.0, 29.9, 29.9, 29.9, 29.9, 29.8, 29.7, 29.6, 29.5, 26.3, 26.1, 22.9, 22.9, 14.2, 14.2 ppm; FTIR (ATR): $\tilde{\nu}$=2921 (C–H alkyl), 2852 (C–H alkyl), 1671 (amide C=O), 1567 (amide N–H), 1510 (aromatic), 1493 (aromatic), 1467, 1445, 1428, 1370, 1330, 1296 (amide C–N), 1239, 1201, 1118, 1074, 1029, 1005, 945, 913, 863, 799, 745, 729, 717, 696 cm^{-1}; UV/Vis (dodecane, 17 mM, 25 °C): λ_{max} (ε)=209 (94.9×10^3), 294 (62.3×10^3), 353 (shoulder, 31.5×10^3), 364 (36.1×10^3), 383 nm (25.2×10^3 M^{-1} cm^{-1}); UV/Vis (chloroform, 19 mM, 25 °C): λ_{max} (ε)=293 (83.2×10^3), 341 (shoulder, 48.6×10^3), 352 (51.9×10^3), 366 nm (shoulder, 34.2×

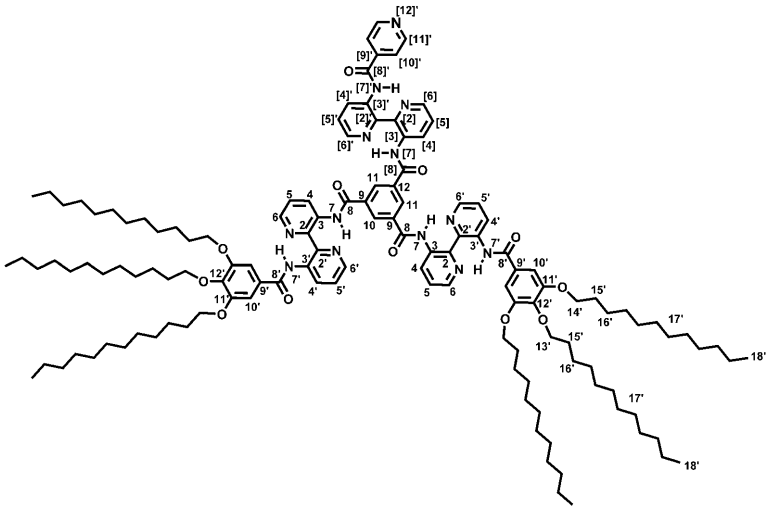

$10^3\,M^{-1}cm^{-1}$); MALDI-TOF MS: *m/z*: calcd: 2133.43; found: 2134.26 [*M*+H$^+$], 2156.48 [*M*+Na$^+$], 2172.47 [*M*+K$^+$], 2197.29 [*M*+Cu$^+$]; elemental analysis calcd (%) for $C_{131}H_{185}N_{13}O_{12}$: C 73.73, H 8.74, N 8.53; found: C 73.65, H 8.63, N 8.51.

Acknowledgements

We thank Dr. Xianwen Lou for the MALDI-TOF MS measurements, Henk Eding for performing elemental analysis, Chunxia Sun for performing TGA measurements, and Ralf Bovee for helping with the (recycling) GPC measurements. Jolanda Spiering is acknowledged for the synthesis of 3,4,5-tris[(*S*)-3,7-dimethyloctyloxy]benzoic acid, and Martijn Veld for the artwork in Figure 1. We thank Professors J. Barberá and W. de Jeu for providing us access to their X-ray diffraction equipment at, respectively, the University of Zaragoza (ES) and the FOM institute (NL); and Dr. D. Byelov for his assistance with the latter one. R.M.R. acknowledges support from an EU Marie Curie Intra-European Fellowship (project MEIF-CT-2006-042044) within the EC Sixth Framework Programme. This work was financially supported by the NRSC-Catalysis Institute.

[1] T. Metzroth, A. Hoffmann, R. Martín-Rapún, M. M. J. Smulders, K. Pieterse, A. R. A. Palmans, J. A. J. M. Vekemans, E. W. Meijer, H.-W. Spiess, J. Gauss, unpublished results.

[2] a) S. Chandrasekhar, B. K. Sadashiva, K. A. Suresh, *Pramana* **1977**, *9*, 471–480; b) D. Demus, J. Goodby, G. W. Gray, H. W. Spiess, V. Vill, S. Chandrasekhar in *Columnar, Discotic Nematic and Lamellar Liquid Crystals: Their Structures and Physical Properties, Vol. 2B*, Wiley-VCH, Weinheim, **1998**, pp. 749–780.

[3] a) S. Laschat, A. Baro, N. Steinke, F. Giesselmann, C. Hägele, G. Scalia, R. Judele, E. Kapatsina, S. Sauer, A. Schreivogel, M. Tosoni, *Angew. Chem.* **2007**, *119*, 4916–4973; *Angew. Chem. Int. Ed.* **2007**, *46*, 4832–4887; b) S. Laschat, A. Baro, N. Steinke, F. Giesselmann, C. Hägele, G. Scalia, R. Judele, E. Kapatsina, S. Sauer, A. Schreivogel, M. Tosoni, *Angew. Chem.* **2007**, *119*, 4916–4973; *Angew. Chem. Int. Ed.* **2007**, *46*, 4832–4887; c) S. Sergeyev, W. Pisula, Y. H. Geerts, *Chem. Soc. Rev.* **2007**, *36*, 1902–1929.

[4] a) L. Schmidt-Mende, A. Fechtenkotter, K. Müllen, E. Moons, R. H. Friend, J. D. MacKenzie, *Science* **2001**, *293*, 1119–1122; b) R. J. Bushby, O. R. Lozman, *Curr. Opin. Colloid Interface Sci.* **2002**, *7*, 343–354; c) R. Schmidt, J. H. Oh, Y.-S. Sun, M. Deppisch, A.-M. Krause, K. Radacki, H. Braunschweig, M. Könemann, P. Erk, Z. Bao, F. Würthner, *J. Am. Chem. Soc.* **2009**, *131*, 6215–6228; d) W. Pisula, M. Zorn, J. Y. Chang, K. Müllen, R. Zentel, *Macromol. Rapid Commun.* **2009**, *30*, 1179–1202.

[5] a) S. Kumar, S. K. Varshney, *Angew. Chem.* **2000**, *112*, 3270–3272; *Angew. Chem. Int. Ed.* **2000**, *39*, 3140–3142; b) S. Kumar, S. K. Varshney, *Angew. Chem.* **2000**, *112*, 3270–3272; c) K. Kawata, *Chem. Rec.* **2002**, *2*, 59–80.

[6] P. Herwig, C. W. Kayser, K. Müllen, H. W. Spiess, *Adv. Mater.* **1996**, *8*, 510–513.

[7] a) T. Kato, N. Mizoshita, K. Kishimoto, *Angew. Chem.* **2006**, *118*, 44–74; *Angew. Chem. Int. Ed.* **2006**, *45*, 38–68; b) T. Kato, N. Mizoshita, K. Kishimoto, *Angew. Chem.* **2006**, *118*, 44–74; *Angew. Chem. Int. Ed.* **2006**, *45*, 38–68.

[8] a) J. Barberá, R. Iglesias, J. L. Serrano, T. Sierra, M. R. de La Fuente, B. Palacios, M. A. Pérez-Jubindo, J. T. Vázquez, *J. Am. Chem. Soc.* **1998**, *120*, 2908–2918; b) J. Barberá, A. Elduque, R. Giménez, F. J. Lahoz, J. A. López, L. A. Oro, J. L. Serrano, *Inorg. Chem.* **1998**, *37*, 2960–2967.

[9] J. Barberá, E. Cavero, M. Lehmann, J. L. Serrano, T. Sierra, J. T. Vázquez, *J. Am. Chem. Soc.* **2003**, *125*, 4527–4533.

[10] T. Kato, T. Yasuda, Y. Kamikawa, M. Yoshio, *Chem. Commun.* **2009**, 729–739.

[11] a) F. J. M. Hoeben, P. Jonkheijm, E. W. Meijer, A. P. H. J. Schenning, *Chem. Rev.* **2005**, *105*, 1491–1546; b) Z. Chen, A. Lohr, C. R. Saha-Moller, F. Würthner, *Chem. Soc. Rev.* **2009**, *38*, 564–584.

[12] a) C. F. van Nostrum, A. W. Bosman, G. H. Gelinck, S. J. Picken, P. G. Schouten, J. M. Warman, A. J. Schouten, R. J. M. Nolte, *J. Chem. Soc. Chem. Commun.* **1993**, 1120–1122; b) A. R. A. Palmans, E. W. Meijer, *Angew. Chem.* **2007**, *119*, 9106–9126; *Angew. Chem. Int. Ed.* **2007**, *46*, 8948–8968; c) A. R. A. Palmans, E. W. Meijer, *Angew. Chem.* **2007**, *119*, 9106–9126; *Angew. Chem. Int. Ed.* **2007**, *46*, 8948–8968; d) F. Vera, J. L. Serrano, T. Sierra, *Chem. Soc. Rev.* **2009**, *38*, 781–796.

[13] a) Y. Matsunaga, N. Miyajima, Y. Nakayasu, S. Sakai, M. Yonenaga, *Bull. Chem. Soc. Jpn.* **1988**, *61*, 207–210; b) M. P. Lightfoot, F. S. Mair, R. G. Pritchard, J. E. Warren, *Chem. Commun.* **1999**, 1945–1946; c) M. M. J. Smulders, A. P. H. J. Schenning, E. W. Meijer, *J. Am. Chem. Soc.* **2008**, *130*, 606–611.

[14] P. J. M. Stals, M. M. J. Smulders, R. Martín-Rapún, A. R. A. Palmans, E. W. Meijer, *Chem. Eur. J.* **2009**, *15*, 2071–2080.

[15] A. R. A. Palmans, J. A. J. M. Vekemans, E. W. Meijer, *Recl. Trav. Chim. Pays-Bas* **1995**, *114*, 277–284.

[16] A. R. A. Palmans, J. A. J. M. Vekemans, H. Fischer, R. A. Hikmet, E. W. Meijer, *Chem. Eur. J.* **1997**, *3*, 300–307.

[17] a) A. R. A. Palmans, J. A. J. M. Vekemans, E. E. Havinga, E. W. Meijer, *Angew. Chem.* **1997**, *109*, 2763–2765; *Angew. Chem. Int. Ed. Engl.* **1997**, *36*, 2648–2651; b) A. R. A. Palmans, J. A. J. M. Vekemans, E. E. Havinga, E. W. Meijer, *Angew. Chem.* **1997**, *109*, 2763–2765; *Angew. Chem. Int. Chem.* **1997**, *36*, 2648–2651.

[18] a) L. Brunsveld, H. Zhang, M. Glasbeek, J. A. J. M. Vekemans, E. W. Meijer, *J. Am. Chem. Soc.* **2000**, *122*, 6175–6182; b) L. Brunsveld, B. G. G. Lohmeijer, J. A. J. M. Vekemans, E. W. Meijer, *J. Inclusion Phenom. Macrocyclic Chem.* **2001**, *41*, 61–64.

[19] L. Brunsveld, J. A. J. M. Vekemans, H. M. Janssen, E. W. Meijer, *Mol. Cryst. Liq. Cryst.* **1999**, *331*, 2309–2316.

[20] M. M. Green, M. P. Reidy, R. D. Johnson, G. Darling, D. J. O'Leary, G. Willson, *J. Am. Chem. Soc.* **1989**, *111*, 6452–6454.

[21] L. Brunsveld, B. G. G. Lohmeijer, J. A. J. M. Vekemans, E. W. Meijer, *Chem. Commun.* **2000**, 2305–2306.

[22] a) M. M. Green, B. A. Garetz, B. Munoz, H. Chang, S. Hoke, R. G. Cooks, *J. Am. Chem. Soc.* **1995**, *117*, 4181–4182; b) J. van Gestel, A. R. A. Palmans, B. Titulaer, J. A. J. M. Vekemans, E. W. Meijer, *J. Am. Chem. Soc.* **2005**, *127*, 5490–5494.

[23] a) I. Danila, F. Riobé, J. Puigmartí-Luis, A. P. del Pino, J. D. Wallis, D. B. Amabilino, N. Avarvari, *J. Mater. Chem.* **2009**, *19*, 4495–4504; b) M. K. Müller, L. Brunsveld, *Angew. Chem.* **2009**, *121*, 2965–2968; *Angew. Chem. Int. Ed.* **2009**, *48*, 2921–2924.

[24] a) A. Kettner, J. H. Wendorff, *Liq. Cryst.* **1999**, *26*, 483–487; b) J. J. van Gorp, J. A. J. M. Vekemans, E. W. Meijer, *Mol. Cryst. Liq. Cryst.* **2003**, *397*, 491–505; c) J. Babuin, E. J. Foster, V. E. Williams, *Tetrahedron Lett.* **2003**, *44*, 7003–7005; d) M. Lehmann, R. Gearba, D. Ivanov, M. H. J. Koch, *Mol. Cryst. Liq. Cryst.* **2004**, *411*, 397–406; e) E. J. Foster, R. B. Jones, C. Lavigueur, V. E. Williams, *J. Am. Chem. Soc.* **2006**, *128*, 8569–8574; f) H. Bock, M. Rajaoarivelo, S. Clavaguera, E. Grelet, *Eur. J. Org. Chem.* **2006**, 2889–2893; g) S. C. Chien, H. H. Chen, H. C. Chen, Y. L. Yang, H. F. Hsu, T. L. Shih, J. J. Lee, *Adv. Funct. Mater.* **2007**, *17*, 1896–1902; h) A. N. Cammidge, A. R. Beddall, H. Gopee, *Tetrahedron Lett.* **2007**, *48*, 6700–6703; i) C. W. Ong, J. Y. Hwang, M. C. Tzeng, S. C. Liao, H. F. Hsu, T. H. Chang, *J. Mater. Chem.* **2007**, *17*, 1785–1790; j) M. Lehmann, M. Jahr, *Chem. Mater.* **2008**, *20*, 5453–5456; k) C. Lavigueur, E. J. Foster, V. E. Williams, *J. Am. Chem. Soc.* **2008**, *130*, 11791–11800; l) M. M. Elmahdy, X. Dou, M. Mondeshki, G. Floudas, H.-J. Butt, H. W. Spiess, K. Müllen, *J. Am. Chem. Soc.* **2008**, *130*, 5311–5319; m) C. W. Ong, C.-Y. Hwang, S.-C. Liao, C.-H. Pan, T.-H. Chang, *J. Mater. Chem.* **2009**, *19*, 5149–5154; n) E. Voisin, E. J. Foster, M. Rakotomalala, V. E. Williams, *Chem. Mater.* **2009**, *21*, 3251–3261.

[25] a) S. Kumar, M. Manickam, H. Schönherr, *Liq. Cryst.* **1999**, *26*, 1567–1571; b) P. H. J. Kouwer, W. F. Jager, W. J. Mijs, S. J. Picken, *J. Mater. Chem.* **2003**, *13*, 458–469; c) E. J. Foster, C. Lavigueur, Y. C. Ke, V. E. Williams, *J. Mater. Chem.* **2005**, *15*, 4062–4068; d) A. Kohl-

meier, D. Janietz, *Liq. Cryst.* **2007**, *34*, 289–294; e) A. de La Escosura, M. V. Martínez-Diaz, J. Barberá, T. Torres, *J. Org. Chem.* **2008**, *73*, 1475–1480; f) C. F. C. Fitié, I. Tomatsu, D. Byelov, W. H. de Jeu, R. P. Sijbesma, *Chem. Mater.* **2008**, *20*, 2394–2404; g) A. Kohlmeier, A. Nordsieck, D. Janietz, *Chem. Mater.* **2009**, *21*, 491–498.

[26] a) F. Camerel, L. Bonardi, G. Ulrich, L. Charbonniere, B. Donnio, C. Bourgogne, D. Guillon, P. Retailleau, R. Ziessel, *Chem. Mater.* **2006**, *18*, 5009–5021; b) F. Camerel, L. Bonardi, M. Schmutz, R. Ziessel, *J. Am. Chem. Soc.* **2006**, *128*, 4548–4549.

[27] a) J. P. Hill, W. Jin, A. Kosaka, T. Fukushima, H. Ichihara, T. Shimomura, K. Ito, T. Hashizume, N. Ishii, T. Aida, *Science* **2004**, *304*, 1481–1483; b) W. Jin, T. Fukushima, M. Niki, A. Kosaka, N. Ishii, T. Aida, *Proc. Natl. Acad. Sci. USA* **2005**, *102*, 10801–10806; c) W. Jin, T. Fukushima, A. Kosaka, M. Niki, N. Ishii, T. Aida, *J. Am. Chem. Soc.* **2005**, *127*, 8284–8285; d) Y. Yamamoto, T. Fukushima, W. Jin, A. Kosaka, T. Hara, T. Nakamura, A. Saeki, S. Seki, S. Tagawa, T. Aida, *Adv. Mater.* **2006**, *18*, 1297–1300; e) Y. Yamamoto, T. Fukushima, A. Saeki, S. Seki, S. Tagawa, N. Ishii, T. Aida, *J. Am. Chem. Soc.* **2007**, *129*, 9276–9277; f) J. L. Mynar, T. Yamamoto, A. Kosaka, T. Fukushima, N. Ishii, T. Aida, *J. Am. Chem. Soc.* **2008**, *130*, 1530–1531.

[28] B. El Hamaoui, L. Zhi, W. Pisula, U. Kolb, J. Wu, K. Müllen, *Chem. Commun.* **2007**, 2384–2386.

[29] a) J. Y. Chang, J. H. Baik, C. B. Lee, M. J. Han, S.-K. Hong, *J. Am. Chem. Soc.* **1997**, *119*, 3197–3198; b) I. H. Hwang, S. J. Lee, J. Y. Chang, *J. Polym. Sci. Polym. Chem. Ed.* **2003**, *41*, 1881–1891; c) A. J. Wilson, M. Masuda, R. P. Sijbesma, E. W. Meijer, *Angew. Chem.* **2005**, *117*, 2315–2319; *Angew. Chem. Int. Ed.* **2005**, *44*, 2275–2279; d) A. J. Wilson, M. Masuda, R. P. Sijbesma, E. W. Meijer, *Angew. Chem.* **2005**, *117*, 2315–2319; *Angew. Chem. Int. Ed.* **2005**, *44*, 2275–2279; e) T. Yamamoto, T. Fukushima, Y. Yamamoto, A. Kosaka, W. Jin, N. Ishii, T. Aida, *J. Am. Chem. Soc.* **2006**, *128*, 14337–14340.

[30] T. Ishi-i, R. Kuwahara, A. Takata, Y. Jeong, K. Sakurai, S. Mataka, *Chem. Eur. J.* **2006**, *12*, 763–776.

[31] a) B. Q. Wang, K. Q. Zhao, P. Hu, W. H. Yu, C. Y. Gao, Y. Shimizu, *Mol. Cryst. Liq. Cryst.* **2007**, *479*, 1173–1188; b) X. Dou, W. Pisula, J. Wu, G. J. Bodwell, K. Müllen, *Chem. Eur. J.* **2008**, *14*, 240–249.

[32] T. Vilaivan, *Tetrahedron Lett.* **2006**, *47*, 6739–6742.

[33] Eluent: chloroform, column: 2×PL gel 3 mm 100 Å columns.

[34] Usage of thionyl chloride causes some chlorination on the aromatic moiety, which can be prevented by using oxalyl chloride.

[35] H. N. Wingfield, W. R. Harlan, H. R. Hanmer, *J. Am. Chem. Soc.* **1953**, *75*, 4364–4364.

[36] a) J. J. van Gorp, J. A. J. M. Vekemans, E. W. Meijer, *J. Am. Chem. Soc.* **2002**, *124*, 14759–14769; b) E. Wuckert, S. Laschat, A. Baro, C. Hägele, F. Giesselmann, H. Luftmann, *Liq. Cryst.* **2006**, *33*, 103–107.

[37] C. Destrade, P. Foucher, H. Gasparoux, N. H. Tinh, A. M. Levelut, J. Malthete, *Mol. Cryst. Liq. Cryst.* **1984**, *106*, 121–146.

[38] K. Kishikawa, S. Nakahara, Y. Nishikawa, S. Kohmoto, M. Yamamoto, *J. Am. Chem. Soc.* **2005**, *127*, 2565–2571.

[39] Due to poor thermal isolation in the Linkam heat stage, compared to the DSC the transition temperature will differ.

[40] D. M. Collard, C. P. Lillya, *J. Am. Chem. Soc.* **1991**, *113*, 8577–8583.

[41] a) S. J. Cross, J. W. Goodby, A. W. Hall, M. Hird, S. M. Kelly, K. J. Toyne, C. Wu, *Liq. Cryst.* **1998**, *25*, 1–11; b) X. L. Feng, W. Pisula, M. Ai, S. Groper, J. P. Rabe, K. Müllen, *Chem. Mater.* **2008**, *20*, 1191–1193.

[42] A. M. Levelut, *J. Phys. Lett.* **1979**, *40*, L81–L84.

[43] J. Barberá, L. Puig, P. Romero, J. L. Serrano, T. Sierra, *J. Am. Chem. Soc.* **2006**, *128*, 4487–4492.

[44] a) E. Fontes, P. A. Heiney, W. H. de Jeu, *Phys. Rev. Lett.* **1988**, *61*, 1202; b) J. Wu, M. D. Watson, K. Müllen, *Angew. Chem.* **2003**, *115*, 5487–5491; *Angew. Chem. Int. Ed.* **2003**, *42*, 5329–5333; c) J. Wu, M. D. Watson, K. Müllen, *Angew. Chem.* **2003**, *115*, 5487–5491; *Angew. Chem.* **2003**, *42*, 5329–5333; d) M. Lehmann, G. Kestemont, R. G. Aspe, C. Buess-Herman, M. H. J. Koch, M. G. Debije, J. Piris, M. P. de Haas, J. M. Warman, M. D. Watson, V. Lemaur, J. Cornil, Y. H. Geerts, R. Gearba, D. A. Ivanov, *Chem. Eur. J.* **2005**, *11*, 3349–3362; e) F. Nolde, W. Pisula, S. Müller, C. Kohl, K. Müllen, *Chem. Mater.* **2006**, *18*, 3715–3725; f) J. Barberá, J. Jimenez, A. Laguna, L. Oriol, S. Pérez, J. L. Serrano, *Chem. Mater.* **2006**, *18*, 5437–5445; g) W. Pisula, Ž. Tomović, M. D. Watson, K. Müllen, J. Kussmann, C. Ochsenfeld, T. Metzroth, J. Gauss, *J. Phys. Chem. B* **2007**, *111*, 7481–7487; h) M. Peterca, V. Percec, M. R. Imam, P. Leowanawat, K. Morimitsu, P. A. Heiney, *J. Am. Chem. Soc.* **2008**, *130*, 14840–14852; i) X. L. Feng, W. Pisula, M. Takase, X. Dou, V. Enkelmann, M. Wagner, N. Ding, K. Müllen, *Chem. Mater.* **2008**, *20*, 2872–2874.

[45] M. M. Green, N. C. Peterson, T. Sato, A. Teramoto, R. Cook, S. Lifson, *Science* **1995**, *268*, 1860–1866.

[46] M. Kastler, W. Pisula, D. Wasserfallen, T. Pakula, K. Müllen, *J. Am. Chem. Soc.* **2005**, *127*, 4286–4296.

[47] a) S. Y. Ryu, S. Kim, J. Seo, Y.-W. Kim, O.-H. Kwon, D.-J. Jang, S. Y. Park, *Chem. Commun.* **2004**, 70–71; b) J. Seo, S. Kim, S. H. Gihm, C. R. Park, S. Y. Park, *J. Mater. Chem.* **2007**, *17*, 5052–5057.

[48] a) P. Toele, J. J. van Gorp, M. Glasbeek, *J. Phys. Chem. A* **2005**, *109*, 10479–10487; b) K. L. Genson, J. Holzmueller, M. Ornatska, Y.-S. Yoo, M.-H. Par, M. Lee, V. V. Tsukruk, *Nano Lett.* **2006**, *6*, 435–440.

[49] Instead of heptane, dodecane is used for these spectroscopic measurements due to its higher boiling point.

[50] L. Kaczmarek, P. Nantka-Namirski, *Acta Pol. Pharm.* **1979**, *36*, 629–634.

[51] Heating of a TFA salt of an amine can cause the formation of a TFA amide.

Received: October 30, 2009
Published online: December 22, 2009

